TRIBHUVAN UNIVERSITY

INSTITUTE OF ENGINEERING

PULCHOWK CAMPUS

THESIS NO: M-58-MSMDE-2019-2022

Modeling, Simulation and Thermal Analysis of the Electric Resistance Furnace used in the Heat Treatment of Clay Based Ceramics

by

Binod Adhikari

A THESIS

SUBMITTED TO THE DEPARTMENT OF MECHANICAL AND AEROSPACE ENGINEERING IN PARTIAL FULFILLMENT OF THE REQUIREMENTS FOR THE DEGREE OF MASTER OF SCIENCE IN MECHANICAL SYSTEMS DESIGN ENGINEERING

DEPARTMENT OF MECHANICAL AND AEROSPACE ENGINEERING

LALITPUR, NEPAL

September, 2022

COPYRIGHT

TRIBHUVAN UNIVERSITY

INSTITUTE OF ENGINEERING

PULCHOWK CAMPUS

DEPARTMENT OF MECHANICAL AND AEROSPACE ENGINEERING

The undersigned certify that they have read, and recommend to the Institute of Engineering for acceptance, a thesis entitled "**Modeling, Simulation and Thermal Analysis of Electric Resistance Furnace used in the Heat Treatment of Clay Based Ceramics.**" submitted by Mr. Binod Adhikari (PUL075MSMDE008) in partial fulfilment of the requirements for the degree of Masters of Science in Mechanical Systems Design Engineering.

_____

Supervisor, Prof. Dr. Rajendra Shrestha
Department of Mechanical and
Aerospace Engineering, Pulchowk Campus

_____

External Examiner, Senior Lecturer
Er. Surya Man Koju
Khwopa Engineering College

_____

Committee Chairperson, Dr. Surya Prasad Adhikari
Head, Department of Mechanical and Aerospace
Engineering, Pulchowk Campus

Date: 16th September, 2022

ABSTRACT

Electric resistance furnace is an improved type of furnace than the fuel fired furnaces that operate with the aid of electricity. In this type of furnace, the desired temperature inside the furnace for heat treatment of clay based ceramics is obtained by the use of a heating element which generates heat based on the Joules law of heating. Electric resistance furnace can replace the traditional fuel fired furnace in the pottery and ceramic industry as these furnaces utilize the electricity to heat treat the clay based ceramics in a more uniform manner. Any attempt to preserve the heat or minimize the losses would result in an increased efficiency of the furnace and hence the subsequent energy saving. In this study, an electric resistance furnace is modeled and an attempt to study the thermal behaviour of the furnace is made. The temperature distribution in the walls, the furnace internal environment and the material to be treated are the scope of this study. The results were then verified with the experimental data obtained from the field visit for the outer wall temperature and the furnace internal temperature. Computational study show the temperature deviation on the walls of the furnace below 14% and internal temperature below 5% than that of the experimental value. Further, an attempt to reduce the external wall temperature and heat flux is made by certain variations in the insulating material. The alteration of the insulation by constant total thickness method adopted reduces the heat flux by 29.4% while for meeting the industrial standards, minimum addition of 40mm of insulation is needed. The study is aimed to provide optimum design for reconstruction of the worn out furnaces as well as the improved future designs of the furnace.

ACKNOWLEDGEMENTS

I would like to express my profound appreciation and sincere thanks to Prof. Dr. Rajendra Shrestha, my thesis supervisor, for his professional advice, constant support and recommendations when required, and unwavering encouragement during the research period.

I would also want to thank the Department of Mechanical and Aerospace Engineering, as well as the Institute of Engineering, for their help with the thesis. Dr. Surya Prasad Adhikari, Head of Department of Mechanical and Aerospace Engineering, Pulchowk Campus, has my gratitude for his assistance and advice. I would like to thank Prof. Dr. Laxman Poudel, MSMDE coordinator, for building an amazing interactive environment for thesis work, as well as the complete elite committee members for their helpful remarks and advice that helped to make this work more relevant. I would want to thank Asst. Prof. Kamal Darlami and Asst. Prof. Bijendra Prajapati for their constant guide and support during this study. I would also like to thank every one of my 075MSMDE co-workers for their constant support, thoughts, and recommendations.

I would also want to offer my heartfelt gratitude and appreciation to my parents, family members and friends for their unwavering support and constant source of inspiration during this thesis project.

TABLE OF CONTENTS

LIST OF FIGURES

LIST OF TABLES

NOMENCLATURE OF SYMBOLS

V : Voltage

I : Current

R : Resistance

P : Power

k : Thermal conductivity

$\dot{e}_{gen}$: Energy generated per unit volume

α : Thermal diffusivity

x, y, z : Cartesian co-ordinates

Q_c : Heat transfer due to conduction

Q_h : Heat transfer due to convection

q'' : Heat flux

ν : Kinetic viscosity

n : Unit normal vector

T_s : Surface temperature of the furnace

T_∞ : Ambient temperature

α : Thermal diffusivity

α_s : Temperature coefficient of resistance

ϵ_i : Emissivity of ceramic fire blanket

ρ_S : Mass density of the solid

T_{iw} : Temperature of workpiece

$T_{\infty i}$: Temperature of the internal environment of furnace

Ra : Rayleigh Number

Nu : Nusselt Number

Pr : Prandtl Number

Gr : Grasshoff Number

c_{pa} : Specific heat of air

c_{pr} : Specific heat of refractory brick

c_{pi} : Specific heat of insulation

c_{pc} : Specific heat of the ceramics

CHAPTER ONE: INTRODUCTION

1.1 Background

The technology of heat treatment of various metals, non-metals and other substances in a furnace is being improved every day. One such improvement is the replacement of direct heating of the workpiece or the working fluid by the burning of fuel with the electrical energy in an electric resistance furnace.

An electric resistance furnace works on the principle of Joules' law of heating. The passage of current through a heating element of certain resistance for a certain amount of time develops heat energy in the heating element. This heat energy is utilized to heat treat the desired product directly or indirectly. In the direct method of heating, current is passed through the workpiece while in the indirect method, the heating elements and workpiece to be heated are put inside an enclosure in which the heat is transferred from the heating element to the workpiece mostly by radiation and convection. Compared to the direct burning of the fuel which release the harmful gases as well as the loss of heat in the flue gases, electrical energy is a cleaner form of energy. This replacement of conventional burning of fuel by the electrical energy has found its application in the pottery and ceramics industry in Nepal as well.

Electrical resistance furnaces have replaced the traditional method of heat treating the ceramics in fuel fired furnaces and oven at various locations inside the Kathmandu valley. Pottery and ceramics production have been associated with the culture and tradition of especially the Newari community. The modernization of the method of heat treatment of ceramics using electrical resistance furnace does not hamper the tradition of local people and hence these people have heartily accepted its use. Pottery and ceramics production in Nepal is not done in large industrial scale and hence there are no any continuous furnaces, instead there are batch furnaces that operate in cycles of heating and subsequent cooling.

The clay based ceramic production in Nepal can benefit a lot from the modernization and improvement of the electric resistance furnaces. The minimum consumption of energy and minimum loss associated with the furnace during its operation leading to the cost effectiveness of the overall heat treatment process are the main desirable features in the electrical resistance furnaces.

1.2 Problem Statement

The start of the use of electrical resistance furnaces in the production of clay based ceramics began the process of modernization in the traditional method of the firing of the ceramics products. There are locations inside the valley where the conventional fuel fired furnaces are still in use but the replacement of the conventional method of firing the ceramics in kilns using fossil fuel, firewood, etc. by firing them in the electric resistance furnaces has led to various advantages. The better control of the firing process and the less periodic inspection of the heat treatment process are its major advantages. Similarly, the heat loss in the flue gas and inspection of the quality of the fuel to be fired have been eliminated. Thus, the use of electric resistance furnaces prove to be convenient. Also, these furnaces are energy efficient and environment friendly.

The cost effectiveness and increase of efficiency of these furnaces by decreasing the heat lost as well as the longevity of the components of the electric resistance heater is a requirement to make people confident in using these furnaces. With the addition of proper operational control features, people will feel confident in using these furnaces. Pottery industry is an energy intensive process. Hence, the study of thermal behavior of the electric resistance furnaces is needed to improve their overall performance, adopt measures of safety, use better building and heating elements as well as to improve their service life by proper operation and maintenance.

1.3 Objectives

The main objective of this research work is to model, simulate and study the heat transfer phenomena of electric resistance furnace and assess the heat loss through the furnace.

The specific objectives of the present research are as follows:

- To design a full scale and simplified CAD models for the existing electric resistance furnace.
- To do a transient study of heat transfer phenomena and study the temperature distribution on the interior of furnace and the furnace walls.
- To analyze the heat and temperature distribution on furnace wall in more detail.

1.4 Assumptions and limitations

The heat transfer process inside the electric resistance furnace is complex conjugate one involving convection and radiation. But due to the limitations in time, suitable measuring instruments and complexity of the process, the following assumptions are made.

- Thermal analysis is done only by taking conduction, convection and radiation separately for the heat transfer process.
- The temperature measured by the thermocouple gives the internal temperature of the environment.
- The heating coil is modelled as thin strips with constant heat flux after attaining a constant temperature.

Besides, the external environmental effects of the furnace operation and effect of furnace on the environment does not fall under the scope of this study. Also, refractory brick layer of wall is assumed a single object and the cementing materials of the walls are not taken into consideration in the study of heat transfer.

CHAPTER TWO: LITERATURE REVIEW

2.1 General Introduction

Electric furnaces were first developed with a view to melting steel commercially by Siemens in 1877 but it did not prove effective. Later, Heroult built arc furnaces using two electrodes and was able to melt the steel and hence commercialize the production of steel(Richards, 2013). Electric resistance furnaces was first devised by Gin, who used a simple rectangular hearth provided with long serpentine groove connected with two heavy terminals and capable of carrying a very heavy current to melt the metal itself. Later Bailey furnace was develop which is a resistance-radiation furnace(Richards, 2013). In this furnace, the metal is heated by radiation from the resistor through which the current is directly passed. A similar type of furnace was Hering furnace in which the liquid metals in small channels communicating with a larger bath of metal, is heated by its own resistance. Induction furnace is also a resistance furnace which was developed by Mr. Colby, of Newark but commercially used by Kjellin in Sweden in 1902(Richards, 2013).

Around the year 1900, W.C. Heraeus, a German-based firm developed the first commercial platinum furnace. In the year 1902, the company marketed a platinum ribbon-bound furnace that could reach a temperature of 1500ºC in 5 minutes, operate at 1500ºC for several hours and could attain a temperature of 1700ºC for brief time periods(Mackenzie, 1982). Since then, the principle of resistive heating remains the same but numerous advancements have been made in the development of electric resistance furnaces in their insulation, control and heating elements.

2.2 Heat treatment of clay based ceramics in furnaces

The clay processing to make different earthen vessels, pottery, is one of the oldest technology known to civilization. Since its discovery during the 10^{th} millennium B.C. in the Sub-Saharan continent, gradual modifications have been made over the course of time. Kilns are basically the container for heat for the shaped earthen vessels, bricks to treat them by heating with the aim to increase their glazing and compressive strength. In 1857, in Germany a continuous brick kiln was invented by F. E. Hoffmann(Awaji et al., 1994). Not much mathematical approach was applied until 1966 by Davies, who gave the basis of calculations in furnace technology. This included the heat energy released by the burning of fuel and the heat energy lost and absorbed by the payload(Davies, 1966).

In Nepal, the challenges & scope of traditional pottery industry was highlighted by (Shrestha, 2018). An approach to study the performance and thermal analysis of fuel fired downdraft kiln was made by (Adhikari et al., 2021) for the sintering process of clay based ceramics. Sintering is the process of heating clay until the particles partially melt and flow together creating a single strong mass composed of glassy phase interspersed with pores and crystalline material. An approach has been made to replace the traditional firewood or fuel fired kilns with the electric resistance furnaces in the Kathmandu valley. However it has been found from literature that no actual mathematical formulation with simulation techniques has been applied to the study of these electric resistance furnaces. This study aims to assess the thermal performance of these furnace walls as well the thermal conditions of the furnace internal environment during operating conditions.

2.3 Types of electric resistance furnaces

Electric resistance furnaces are categorized by a combination of following factors: batch or continuous; protective atmosphere or air atmosphere; method of heat transfer; and operating temperature(C. Barry Carter, 1974).

2.3.1 Batch and continuous furnaces

In batch furnaces, the furnace with the charge to be heat treated are subjected to a particular cycle to accomplish the desired time–temperature cycle for the product. Batch furnaces are mostly used for very large and/or heavy charges and low production rates. The frequency of operation is infrequent, time–temperature cycle is variable, and processing material must be in batches because of previous or subsequent similar operations(Walton, 2000).

2.3.2 Air-atmosphere and protective-atmosphere furnaces

The process requirements of the task will determine whether an electric furnace operates with air inside the furnace or with a protective atmosphere. Air-atmosphere furnaces are used in procedures where the workload can withstand the oxidation that happens when air is heated to a high temperature. When the work cannot sustain oxidation or when the environment has to produce a chemical or metallurgical reaction with the work, protective-atmosphere furnaces are utilized(Walton, 2000). In high temperature applications, the electric heating element needs protective environment to prevent damage from oxidation.

2.3.3 Conduction, convection and radiation furnaces

In conduction furnaces, the heat from the heating elements is transferred to the work being processed by means of a liquid that is heated to its operating temperature. Forced convection is how convection furnaces are intended to transmit the heat from the heating elements. The most typical means of heat transfer in electric resistance furnaces is radiation. In general, a low temperature radiation furnace works below 760 °C, a medium temperature extends from 760 °C to 1050 °C, and high temperature radiation furnaces operate above 1050 °C (Walton, 2000). Internal structural components become crucial in high temperature radiation furnaces, and the insulation system must be able to endure the high temperatures. In order to line the interior of these furnaces, ceramic refractories are necessary.

The type of furnace under study in this paper is high temperature radiation-type, air-atmosphere, chamber electric resistance furnace which operates at around 1050-1200°C for the sintering of the clay based ceramics.

2.4 Components of a high temperature, electric resistance furnace

The major components of a high temperature ERF are; heating element, refractory layer and thermal insulation. Other accessory devices such as pyrometers and thermocouples are needed for measurement of the temperature. Heating elements are the heart of any electric resistance furnaces to produce the desired temperature inside the furnace. The choice of refractory layer, thermal insulation layer and suitable temperature measurement devices are for the proper and efficient operation of the furnace.

2.4.1 Heating element

The type of heating element suitable for a furnace is determined on the basis of the working material, maximum temperature requirements, and the atmosphere inside the furnace. The heating material used in the furnace under study is Kanthal wire which is an alloy of Iron (70-76%), Chromium (20-24%) and Aluminium (4-6%). Different types of elements used as heating element according to the maximum working temperature and usable atmosphere are given in the table below(C. Barry Carter, 1974):

Table 2.1: Different heating elements, their usable temperature and environment

Material	**Maximum useful temperature(°C)**	**Usable atmosphere**
Chrome alloys		
Chromel C, Nichrome, Kanthal DT	1100	ONR
Kanthal A, Chromel A	1300	ONR
Metals		
Pt	1400	ONR
Pt-Rh alloys	1500-1700	ONR
Mo	1800	NR
W	2800	NR
Ceramics		
SiC	1500	ON
MoSi2	1700	ON
Lanthanum chromite	1800	0
Thoria, stabilized	2000	ONR, shock
Zirconia, stabilized	2800	ONR, shock
Graphite	3000	NR

(O, oxidising; N, neutral; R, reducing; Shock, poor resistance to thermal shock)

2.4.2 Refractories

Refractories are materials capable of withstanding high temperatures. They do not degrade in a furnace environment when they come in contact with corrosive liquids and gases. In high-temperature applications, refractory insulators are utilized to cut heat losses and conserve fuel. Based on whether the interior atmosphere of the environment is acidic, basic, or neutral, the refractory materials are chosen. The various refractories are included in the following table along with their maximum operating temperature and thermal conductivity values (Norton & Carter, 2019).

Table 2.2 Different refractory materials, maximum usable temperature and thermal conductivity values

Material	**T_{max}(°C)**	**K ($Wm^{-1}K^{-1}$)**
Glass, fiber	600	0.05
SiO_2	1000	0.17
Firebrick, insulating	1200-1500	0.52
Fiberfrax	1650	0.12
Al_2O_3, bubble	1800	1.04
MgO, powder	2200	0.52
MgO, solid	2300	2.94
Carbon or graphite, powder	3000	0.09
Radiation shields, Mo	2100	0.69

2.4.3 Insulating materials

Insulation is defined as any material, or group of materials, that slows the transfer of heat energy. They aid in lowering heat gain or loss and so improve the system's operational effectiveness. The phrase "thermal insulation" will be used to describe a range of temperatures between -75°C and 815°C. Applications are categorized as "cryogenic" or below -75°C or "refractory" or above 815°C. Fewer materials and application strategies are available as insulation's refractory range is approached. Calcium silicate, cellular glass, cements, ceramic fibres, perlite, glass fibres, and mineral fibres are the most often utilized materials (Ying-Zhang et al., 2013). Ceramic fibre blanket is used as insulation in the furnace under this study, and its thermal conductivity ranges from 0.039 to 0.18 W/(m.K) with the increase of temperature.

2.4.4 Temperature measuring devices

The most common and convenient means of measuring temperature is by the use of thermocouple which works on the principle of Seebeck effect. The thermocouple is not in direct contact with the substrate itself of which the temperature is to be measured, and hence the surface temperature of the heating element can be off by as much as around 100℃ or even more(Norton & Carter, 2019).

The device used to measure the temperature inside the furnace under our study is K type thermocouple which has combination of chromel and alumel alloys and can measure temperature up to 1250℃ (C. Barry Carter, 1974).

2.5 Firing or sintering process

Firing is the process of application of heat to the materials while sintering is the process occurring in the ceramics. A furnace is fired up in three stages.

- The heating-up stage
- The soaking period
- The cooling stage

The variations in the heating-up rate are selected to prevent fractures and pores from forming in the product as a result of the strains brought on by the thermal expansion of the product and the combustion of binders. The maximum heating rate of a furnace is determined by the heating mechanism and furnace design. Temperature and time affect how much sintering occurs. The time the heat-treated material is held at a specific maximum temperature is known as the soaking period. Thermal contraction, crystallization, and other potential phase changes in a product must all be considered throughout the cooling cycle(Carter and Norton, 2019). For many clay-based ceramics, the temperature between 800°C and 600°C is critical during cooling which requires a slower cooling rate to prevent the development of any sort of stress in the product. The total heat treatment curve or sintering curve for the ceramics is as given below (Ferrer et al., 2015).

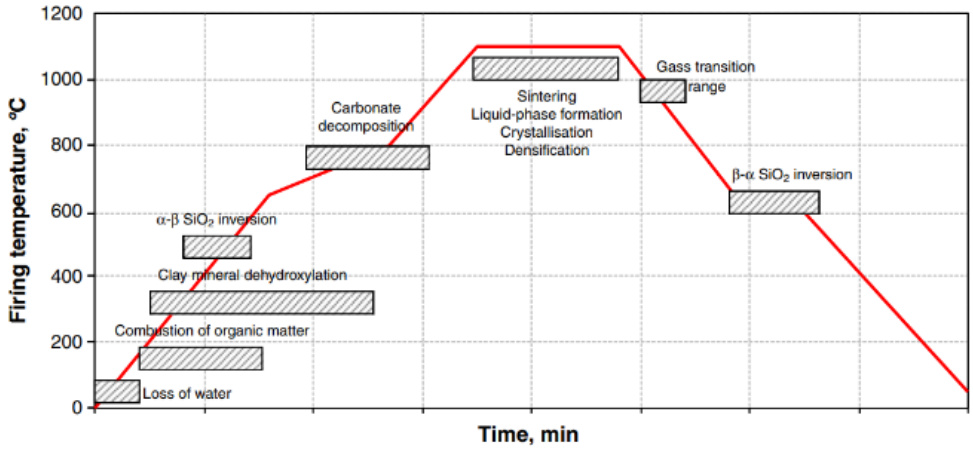

Figure 2.1: A sintering curve for heat treatment of ceramics

The sintering curve for ceramics shows that the downward slope of the curve after reaching the maximum temperature is not steep. This indicates the soaking period for the ceramics. The upward slope of the curve gives the temperature rise rate during the heat treatment process while the downward slope after the soaking temperature gives the rate of cooling. The study in this paper focuses on the temperature rise up to the soaking temperature.

2.6 Previous researches

The need for mathematical modelling was felt for industrial fuel fired furnaces for more economical and rational operation. A simplified attempt of modelling of the complex combustion, fluid flow, heat and mass transfer was made by Janata, in Czechoslovakia (Janata, 1982). The purpose was to satisfactorily describe the real conditions, which can be confirmed by the agreement of the model result with experiments. In 1991, mathematical model of the fluid flow and heat transfer phenomena in an industrial glass furnace was presented (Carvalho & Nogueira, 1991). This model was divided into two sub-models; combustion chamber and glass tank parts to describe the turbulent diffusion flame, soot formation and thermal radiation.

In the year 1995, solution of new time dependent mathematical model for the operation of furnaces involved in the heat treatment and annealing of steel strip was developed by D. Marlow. This mathematical formulation was developed to eliminate the difference between the actual temperature and desired temperature of the steel strip at the edges and hence meet the specified metallurgical requirements (Marlow, 1995).

For an arbitrary shaped workpiece such as a long cylinder or an infinite plate that is heated in a furnace for a given time and temperature, the time for uniform temperature distribution and heating/cooling rates were estimated using improved virtual sphere method based on the conduction in solids (Gao et al., 2000).

The phenomenon of heat transfer through radiation and natural convection in a differentially heated cavity was studied. The radiative transfer equation was solved using the discrete ordinate method (DOM) while the Navier-Stokes (NS) equations were solved with a segregated simple like algorithm. (Colomer et al., 2004).

In 2006, a hybrid method based on numerical simulation and analytical equations was proposed to calculate the radiation, convection and conduction heat transfers in heat treatment processes. The furnace model, radiation model, conduction model and

convection model each were given a separate treatment while studying the overall heat transfer process. (Kang et al., 2006).

Chook and Tan have emphasized that the heating process in an electric resistance furnace is a very complicated process and hence can be treated as either linear or non-linear system. The type of furnace as well as the materials used in the construction, its geometry all should be used to describe the true system(Chook & Tan, 2007). Similarly in 2012, an analysis of the temperature distribution in the workspace of a high temperature chamber type electric resistance furnace was done and a methodology to ensure uniform distribution of temperature field is suggested with the aim of solving technological problem of non-uniform temperature field in such furnaces(Dimitrov & Yatchev, 2012). In 2010, a two dimensional mathematical modelling of the thermal operating regimes of electric resistance furnace was done by Grinchuk. It is shown that the electric resistance furnace's thermal operating efficiency can be improved theoretically by 2 to 2.5 times by replacing the fireclay lining by the lightweight fibrous materials (Grinchuk, 2010).

In 2019, a commercial CFD software, FLUENT was used and numerical analysis of natural convection and surface thermal radiation in a chamber electric furnace that is used to heat treat a superalloy was conducted. This furnace had heat conducting solid walls of finite thickness with a heat source located in the side and top walls of the furnace in conditions of convective heat exchange with the environment has been carried out.(Fu et al., 2019). This model was used to predict the equilibrium time for the superalloy heating.

A numerical simulation of the temperature distribution during the sintering process of ceramics was done by (Zhang et al., 2008). This paper incorporated the effect of radiation to the convective heat transfer coefficient inside the furnace and proposed a simplified model of analysis with the linear sintering curves with different slopes which proves to be erroneous when high temperature is involved.

Attempts in understanding the process inside the chamber of electric resistance furnace and hence its temperature and performance optimization by varying different components were carried out. (Hemmer et al., 2014) showed that the temperature of the box of electric heater increases with the increase in emissivity of the heating element. Similarly, (Ritonga et al., 2021) showed that the temperature inside the electric resistance furnace can be optimized to reach 1200℃ using the Hebel insulation brick. (Dimitrov et al., 2012) did a study to optimize the insulation of industrial grade electric resistance furnace with some

objective functions to minimize weight, volume and price for an allowed range of heat loss through the wall. Similarly, (Dimitrov and Zhekov, 2014) did an analysis of the energy efficiency of the furnaces at the stage of their design as well as the effective methods of reconstruction of the furnaces by replacing the thermal insulation. Results from this study show the decrease in electrical power consumed by the heater. A study on the simulation of sintering was made by (Lin et al., 2011) which showed that the temperature distribution in a large sized object is not uniform and requires a high soaking time to reach the uniform temperature.

In this paper, an effort is made to study in detail the heat transfer process through the wall of the chamber type electric resistance furnace during the second phase of heat treatment of clay based ceramics to around 1150-1200℃. An attempt to study the heat transfer process through the wall of the electric resistance furnace during the furnace's empty operation as well as loaded operation is made with the aim to optimize the performance and suggest future methods to adopt during the construction of new furnaces or the reconstruction of the worn-out furnaces. Firstly, the thermal performance of the existing furnace wall is analysed and then later, a commercially available simulation software package, ANSYS Steady State Thermal and ANSYS Transient Thermal are used to study heat transfer process. The heat transfer process will first be carried out as the steady state thermal analysis to obtain a ballpark value and then later a transient thermal analysis would be carried out.

CHAPTER THREE: METHODOLOGY

In this chapter, the methodology applied for the study from the start to the completion is described. Literature review from different journals, articles and research papers is done for the study of heat treatment of ceramics and the electric resistance furnaces. The experimental data is collected, after which a full scale CAD model is designed of the existing furnace. Then some simplified models are made for the computational study. The boundary conditions are applied and the computational study is carried out. The converged result is interpreted. A comparison with the experimental data is made to carry out the sensitivity analysis. Finally, alternative models to improve the heat transfer loss are proposed with the computational results and then conclusions are drawn. The methodology is as depicted in the following flowchart:

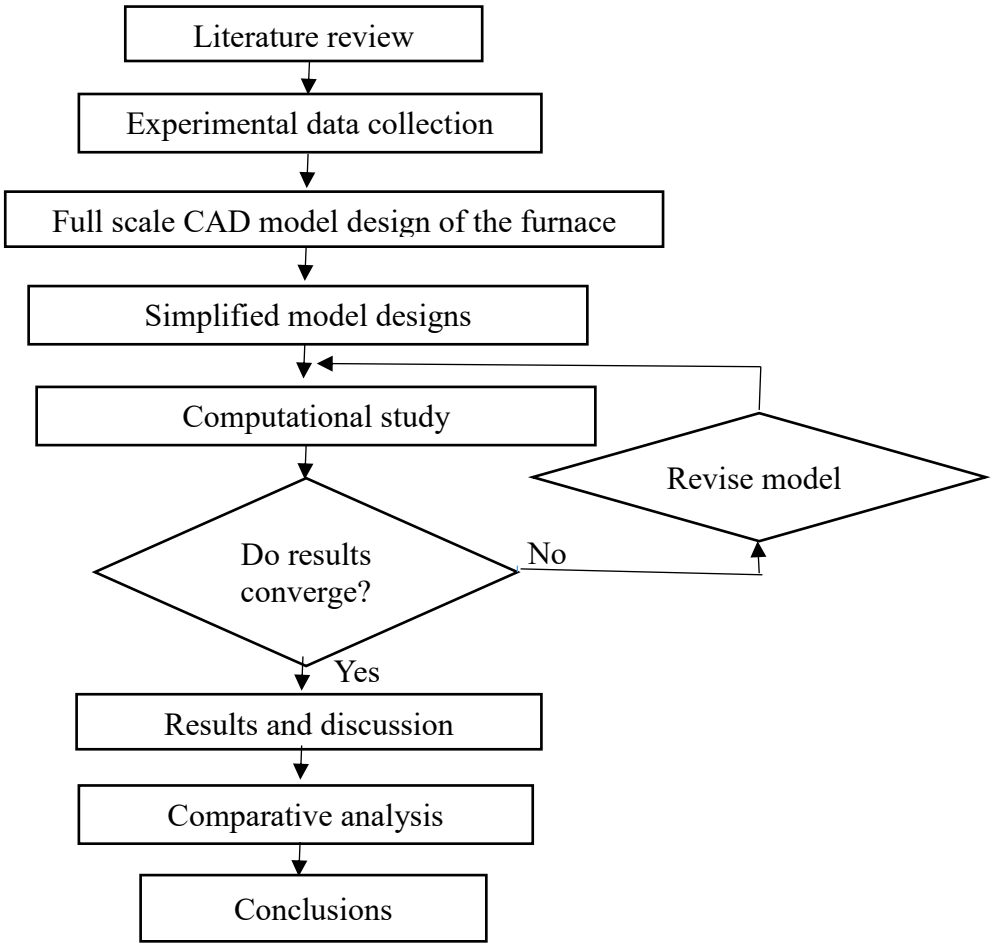

Figure 3.1: Flowchart depicting the methodology adopted in this study

3.1 Literature review

The past works related to electric resistance furnace and its working, sintering process of ceramics, CAD model of the furnace, mathematical formulation and numerical simulation of the heat transfer processes occurring inside different furnace were studied extensively. The review of literature was conducted with the help of internet, books, journals and research paper published earlier. The literature referred were related to doing the performance analysis calculations of the furnaces and different methods of formulating the required equations and hence taking the correct assumptions to model and simulate the heat treatment of the ceramics. Reference had to be taken from many research papers and articles on similar work. The working conditions and the materials used in the construction were studied in detail from different papers available. Literature also suggested that the simulation are carried out using the commercial software such as ANSYS, COMSOL and so on. The development of a 3D CAD model using a designing software and the proper use of the different tools and options in the simulating software is an absolute necessity. The difference in performance during loaded operation and empty operation is tried to be measured by taking a symmetrical object for simulation taking into account the loading considered during experimental study.

3.2 Experimental data collection

The production of pottery and ceramic products has been associated with the Newari community of Kathmandu valley. The data for this study was collected from the Everest Pottery located at Sanothimi, Bhaktapur where a number of electric resistance furnace were installed. The study of this paper focuses on the second firing, also called sintering of the ceramics. The ceramics is heated to a temperature between 1050 and 1200℃ and it takes around 11.5 hours for completion. The K-type thermocouple installed in the furnace measures the internal temperature of the furnace during its operation. A clamp meter is used to measure the current flowing in the wire. A digital infrared thermometer gun was used to measure the outside wall temperature of the furnace. A weighing machine was used to measure the weight of the different clay based ceramics materials to be heat treated before and after the firing process. The dimensions of the furnace and its components were measured using measuring tape and vernier callipers. A special case of loading is considered and weight of all components is measured using weighing machine before the load is put inside the furnace.

3.4 Physical model

A furnace of inner dimensions $920\text{mm} \times 640\text{mm} \times 640\text{mm}$ is considered which has a top opening cover. The cover is 180mm thick and has a layer of insulation only that is reinforced by small wires for mechanical stability. There is uniform insulation of 65 mm on the four walls as well as the bottom of the furnace. The inner wall of the furnace lining is made from refractory brick, outside of which is the layer of insulation. The layer of the refractory brick is 115mm thick while the insulation layer is 65mm thick. Air is the working fluid inside the chamber of electric resistance furnace. The furnace is considered to be high temperature radiation type electric resistance furnace.

3.5 Full scale CAD model design

A full scale CAD model of the electric resistance furnace was designed using the designing software, SOLIDWORKS 2019. For the dimensions of the furnace, the actual measurements were taken using measuring instruments such as measuring tape. This data was verified by inquiry with the local people who purchased the different materials from the suppliers while constructing the furnace. These furnaces were constructed taking a reference of a German company, OEFEN that manufactures different types of heat treatment furnaces. ("Furnaces for Ceramics, Glass Solar Cells," 2021). While for the simulation purpose, symmetry of the furnace was realized and one-eighth section was only taken into consideration. The developed model is used for simulation of the heat transfer by defining the suitable physics and obtaining the necessary boundary and initial conditions.

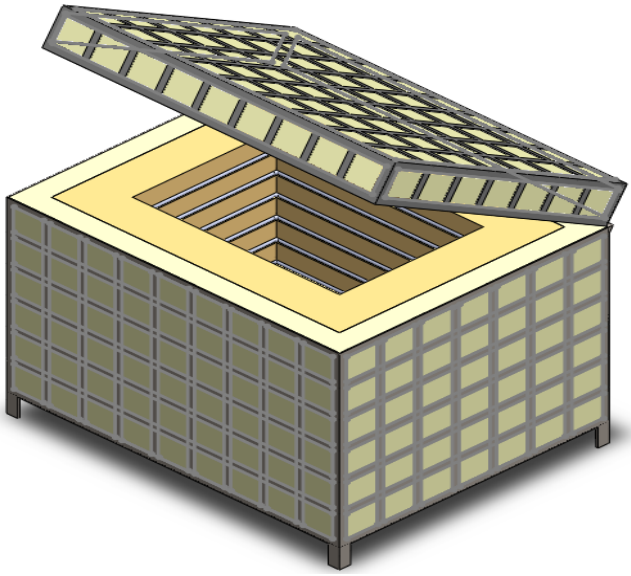

Figure 3.4: Full-scale CAD model of the furnace

3.6 Computational study

Computation software is required to perform the calculations necessary for the simulation of the total heat transfer process through the walls. First, ANSYS Transient Thermal was used to simulate the actual process of the heat transfer during the heat treatment process of the clay based ceramics. Then, ANSYS Steady State Thermal was used to analyse the process of the heat transfer. The various parameters that play a role in the heat transfer process are determined and they are varied one by one to obtain the heat transfer through the wall.

3.7 Relevant heat equations

In resistance furnace, heat conduction happens in the solid zone. The fluid flow happens in the furnace fluid, that is, air. In the solid zone, the heat transfer process is solved by transient heat conduction while in the fluid zone the temperature field is solved by continuity equation, N-S equations as well as the energy equation.

3.7.1 Conduction equations

The general three dimensional transient heat conduction equation in the x, y and z coordinate system or rectangular co-ordinate system is given as:

$$\frac{\partial}{\partial x}\left(k\frac{\partial T}{\partial x}\right)+\frac{\partial}{\partial y}\left(k\frac{\partial T}{\partial y}\right)+\frac{\partial}{\partial z}\left(k\frac{\partial T}{\partial z}\right)+\dot{Q}=\rho c_s\frac{\partial T}{\partial t} \qquad \textit{Equation 3.1}$$

The general three dimensional steady state heat conduction equation in the x, y and z coordinate system or rectangular co-ordinate system is given as:

$$\frac{\partial}{\partial x}\left(k\frac{\partial T}{\partial x}\right)+\frac{\partial}{\partial y}\left(k\frac{\partial T}{\partial y}\right)+\frac{\partial}{\partial z}\left(k\frac{\partial T}{\partial z}\right)+\dot{Q}=0 \qquad \textit{Equation 3.2}$$

In case of isotropic medium or constant thermal conductivity with no heat generation, the equation reduces to:

$$\nabla^2 T=\frac{1}{\alpha}\frac{\partial T}{\partial t} \qquad \textit{Equation 3.3}$$

where α is the thermal diffusivity which is the ratio of thermal and the product of density and specific heat capacity of a substance. This equation is known as Fourier-Biot equation.

The heat conduction for heat flow in three dimensions is given by Fourier law as

$$Q=kA\frac{dT}{dn} \qquad \textit{Equation 3.4}$$

For a layer of walls, the unidimensional heat flux due to conduction can be found by using the formula for steady state conditions.

$$q'' = \frac{T_1 - T_2}{\left(\frac{x_1}{k_1}\right)_A} = \frac{T_2 - T_3}{\left(\frac{x_2}{k_2}\right)_B} = \frac{T_3 - T_4}{\left(\frac{x_3}{k_3}\right)_C} = \frac{T_1 - T_4}{\left(\frac{x_1}{k_1}\right)_A + \left(\frac{x_2}{k_2}\right)_B + \left(\frac{x_3}{k_3}\right)_C} \quad \textit{Equation 3.5}$$

where x and k are the thickness and thermal conductivities of the different wall components.

3.7.2 Convection equations

For natural and free convection, the heat transfer between atmosphere and solid surface by convection is given by

$$Q_h = hA(T_s - T_\infty), h = \frac{k}{L^*} \cdot \bar{N}u_L \quad \textit{Equation 3.6}$$

For chambers or enclosures with no any fans, free convection occurs which may be laminar at lower temperatures and may transition to turbulent at higher temperatures. Since the temperature of the heating element is considered constant, the furnace interior can be modelled as the parallel plates with constant heat source.

The Rayleigh number is a function of Grasshoff number and Prandtl number and is based on the dimension of the enclosure. For Rayleigh number greater than 10^9 the transition occurs from laminar to turbulent. For laminar or turbulent free convection over a vertical plate, that is, for any Rayleigh number, the average Nusselt number is given by

$$Ra = Gr.Pr = \frac{g\beta(T_{iw} - T_{\infty i})L^3}{\nu\alpha} \quad \textit{Equation 3.7}$$

$$\bar{N}u_L = \left\{ 0.825 + \frac{0.387Ra^{\frac{1}{6}}}{\left[1 + \left(\frac{0.492}{Pr}\right)^{\frac{9}{16}}\right]^{\frac{8}{27}}} \right\}^2 \quad \textit{Equation 3.8}$$

3.7.3 Radiation equation

The radiation that occurs through the outer wall of the furnace is calculated using the following relation

$$Q_{rad} = \epsilon_i . A . T_s^4 \quad \textit{Equation 3.9}$$

where ϵ_i is the emissivity of the outer insulation material.

The radiation model inside the furnace is taken to be the surface to surface model and carried out by ANSYS radiosity solver.

3.8 Further analysis of the walls

The following are the deciding parameters for the amount of heat loss through the wall of the chamber type electric resistance furnace by conduction(Indian Bureau of Energy Efficiency, 2015).

- Inside temperature
- Outside temperature
- Thickness of walls
- Conductivity of walls
- Configuration of walls

Apart from conduction, the convection and radiation to some extent occurs from the outer wall of the furnace as well. The convection depends on the environment in which the furnace is placed while the radiation coming out of the furnace depends on the emissivity of the wall of the furnace.

3.9 Documentation and presentation of the findings.

The findings of the research work are presented in the form of conference article and formal thesis report according to the guidelines of the Department of Mechanical and Aerospace Engineering, Pulchowk Campus, Institute of Engineering.

The methodology used for the study of heat transfer process through the walls also includes defining the physical and mathematical model for the present study which were discussed in a detailed manner above.

CHAPTER FOUR: ANALYSIS IN ANSYS

The study of the heat transfer through the furnace wall in ANSYS consists of the following steps: defining the simplified geometric models, describing the physics, initial and necessary boundary conditions, meshing, controlling the parameters affecting the heat transfer, solving and then post-processing the results.

4.1 Simplified model of the furnace wall

The symmetry and regular geometry of the existing furnace wall can be utilized for the easier and faster processing of the problem. One-eighth of the total geometry was considered for the walls, while for the floor and the roof one-fourth of the actual geometry was considered to develop the simplified geometric models. The basic model of the wall is L-shaped that consists of the two layers of refractory brick and a layer of insulation that forms the total wall. The L-shaped geometry is selected to better capture the actual heat transfer process going through the walls. The heating element is modelled as a rectangular strip instead of the coil(Fu et al., 2019). This rectangular strip is modelled as a source of constant heat. The simplified geometric model with dimensions for our study is shown in the Figure 4.1 while the respective dimensions are given in Table 4.1:

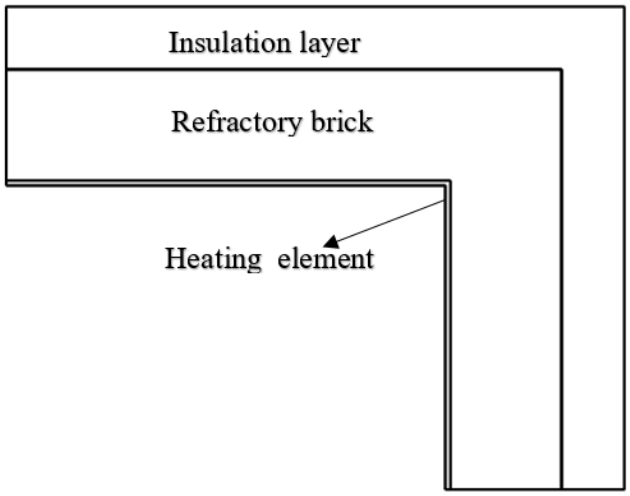

Figure 4.1: Simplified geometric model of the furnace wall

Table 4.1: Dimensions of the different layers for simplified model

Components	Dimensions (m)		
	Length	**Breadth**	**Thickness**
Heating element	0.455	0.315	0.005
Refractory brick	0.575	0.435	0.115
Insulation layer	0.64	0.500	0.06

The thermodynamic property of the different materials used in the construction of the furnace wall are given in the table 4.2 below.

Table 4.2: Thermodynamic properties of existing materials used in the furnace wall

Thermodynamic properties		**Materials**	
	Units	**Refractory brick**	**Ceramic fibre blanket**
Thermal conductivity	J/(kg K)	0.12-0.22	0.039-0.117
Density	kg/m^3	550	128
Heat capacity	W/(m K)	880	1070

4.2 Defining the physics and setup

The simplified model is a multilayered wall in which the heat transfer can be dominantly assumed to be unidirectional. The model is first run under the steady state thermal state to establish the necessary conditions. Then the model is simulated in the transient thermal module with the necessary time stepping. For this time dependent study, the properties of the substance that vary with the temperature are entered in a tabulated form. Since the main aim of the study is to optimize the wall conditions and minimize the outer surface temperature of the furnace wall, a number models of different configurations of the wall are created and the materials are varied. All of these models are simulated in the ANSYS Transient Thermal environment to study the temperature distribution as well as the heat flux through the wall. The material properties are obtained from previous research articles for comparable geometry of the furnace. Some of the initial boundary are found by actual measurement from the site while some are taken from the research articles.(Indian Bureau of Energy Efficiency, 2015). For the study of heat transfer through the walls of the

furnace, the convection coefficient inside the furnace is taken such that it accounts for the radiation occurring inside the chamber furnace (Gołdasz & Malinowski, 2017).

Table 4.3 Boundary conditions and parameters

Parameters	**Value**	**Units**
Outside convection coefficient	5	W/m^2K
External ambient temperature	298	K
Initial internal temperature	298	K
Initial temperature of outside wall	298	K
Thickness of brick layer	0.115	m
Temperature of the heating coil	1573	K
Symmetry boundary condition	0	W
Heat flux emitted by coil	10407	W/m^2
Thickness of insulation	0.065	m

4.3 Meshing

The solution of entire domain in an integral form is impossible, so meshing is the procedure of splitting the computational domain into smaller regions to facilitate the iterative solving of the complex equations by turning them into simple algebraic equations. The preciseness of the solution obtained can be increased by increasing the number mesh elements or sub domains. But very fine meshing requires greater computational time, cost and effort. The finer meshing takes a longer time to generate and hence the total procedure takes more time than is absolutely necessary. So optimum meshing should be done by defining the convergence criterion. In this section, the proper procedure to follow for the meshing is elaborated.

4.3.1 Mesh independence test

The desired preciseness or quality of the output is selected and mesh independence test is done to ensure that the meshing is sufficient to generate the result to this preciseness. The meshing is gradually refined from coarser to finer one by controlling the mesh sizes by controlling various global and local mesh controls. The number of elements and nodes during different conditions of meshing and the desired results for the external wall temperature are as shown in the Table 4.4.

Table 4.4: Mesh independence test

Mesh set	Number		
	Nodes	Elements	Outer furnace wall temperature($°C$)
M1	16602	6532	98.65
M2	43268	15230	97.49
M3	125692	36832	96.98
M4	197171	57223	96.86
M5	345350	99411	96.83

The simulation result was obtained for the high alumina refractory brick having bulk density 550 kg/m^3 for various meshing. The mesh M3, M4 and M5 do not have much variation in the value of temperature at the outer skin of the furnace wall.

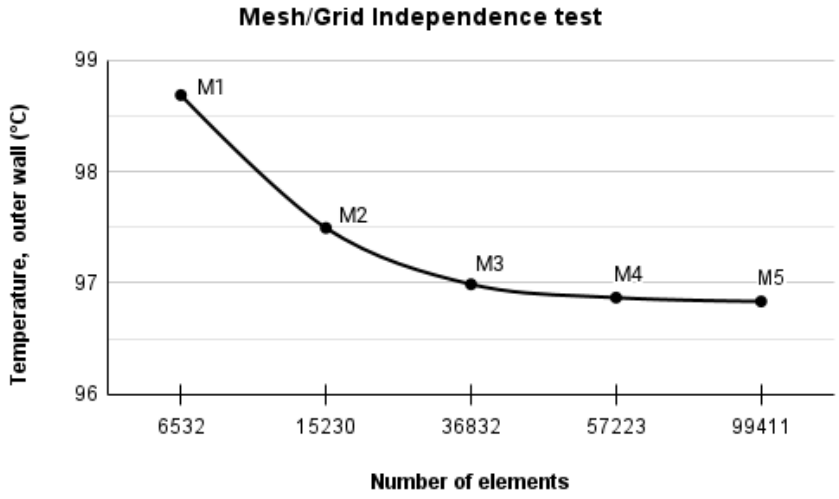

Figure 4.2: Mesh Independence test

Hence the middle mesh set with 197191 number of nodes and 57223 number of elements from M3, M4 and M5, that is, M4 was selected to reduce the computational time and cost.

4.3.2 Mesh generation

The meshing is done in ANSYS 2022 R1 version by controlling the various global and local mesh controls. Global mesh controls such as relevant centre, smoothing and span angle centre are varied for refining process of mesh. The local mesh controls inside the sizing, quality, inflation and others are varied to control the size of the mesh elements. The geometry of our model allowed for different structured as well as unstructured

meshing. The individual components are meshed differently. The area around the heating element is meshed densely than the other areas to capture the heat transfer phenomena more precisely. The meshes of the different layers of the furnace wall is shown in the figure.

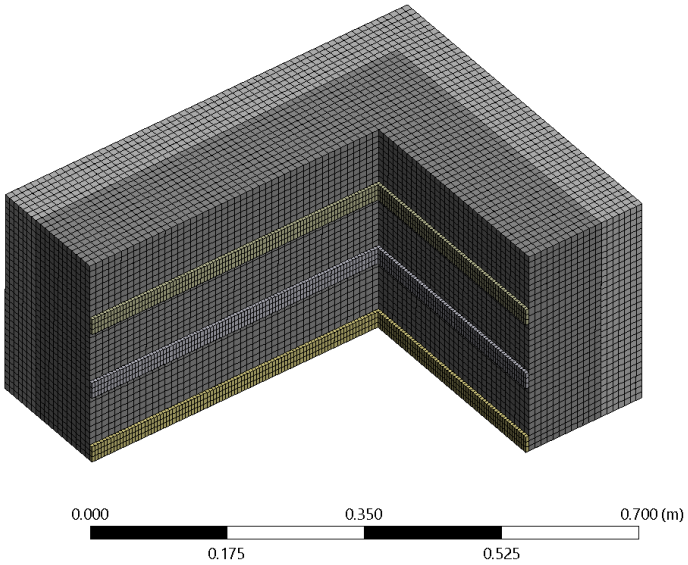

Figure 4.3: Meshing of the simplified model of wall

4.4 Incorporating the fluid domain

After the wall domain has been fully established, a fluid domain is introduced in the inner region of the furnace. The analysis is then done with the fluid domain by applying the initial and necessary boundary conditions.

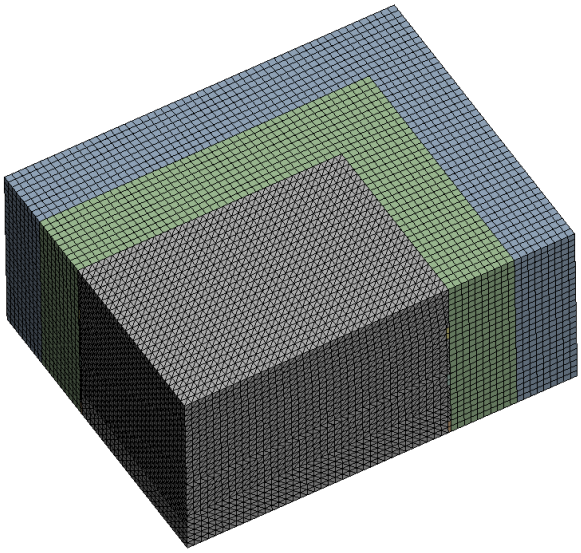

Figure 4.4: Meshing of walls along with the fluid domain

4.5 Incorporating fluid domain and a solid at the centre

After the fluid domain has been incorporated a thin-walled hollow square based object is placed at the centre which has a uniform thickness. The presence of this solid represents the loaded condition of the furnace. Transient thermal analysis is done on this model by applying the necessary and initial boundary conditions.

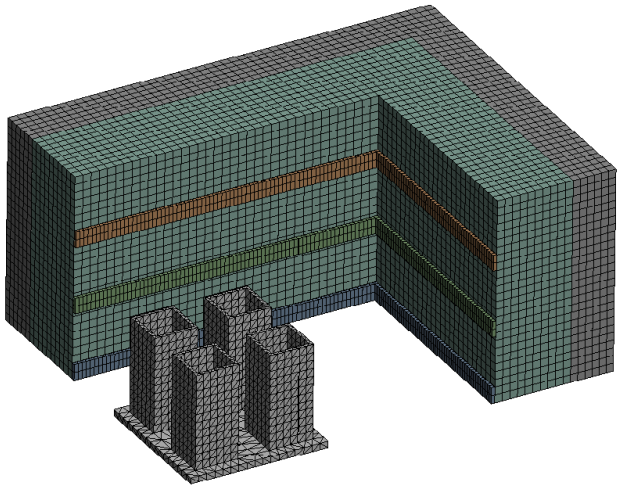

Figure 4.5: Meshing of the walls with fluid domain and solid at the centre

4.7 Solution and post processing

A transient thermal analysis is done to simulate the total heat treatment process with suitable time steps. This is done to simulate the process faster. The heat transfer model is predominantly a one dimensional one because of the symmetry of the walls and the whole furnace. The simulation is done for eleven and a half hours with a first time step of 15 minutes or 900 seconds at first and then every 5400 seconds for the rest of the process. Each of these time steps are further divided into sub-steps of 30 seconds each.

Once the solution converges to the desired value for a given set of dimensions and properties of the material, the temperature distribution, heat flux etc. are obtained during the post processing. The results obtained are either obtained in the plots and graphs or in the form of the data sets which are then plotted to obtain the plots and graphs.

CHAPTER FIVE: RESULTS AND DISCUSSION

The study was carried out in two phases; experimental phase and computational phase. The results of both the phases are as presented below.

5.1 Experimental results

The experimental data was collected from Everest Pottery located at Sanothimi Bhaktapur.

5.1.1 Furnace loading data

The ceramic materials to be heat treated are stacked in two columns by using slabs and blocks. The stacking of the ceramic materials inside the furnace is done in a careful and uniform manner. Each of the components are weighed before stacking inside the furnace.

Table 5.1: Typical case of loading of the furnace

S. No.	Components	Quantity	Weight(kg per piece)	Total weight(kg)
1	Slab	20	7	140
2	Block	54	0.17	9.18
3	Big plate	20	1.118	22.36
4	Small plate	20	0.756	15.12
5	Small disc	80	0.096	7.68
	Total			**194.34**

Out of the 194.34 kg of the loaded material, the actual material to be heat treated are the big plate, small plate and the small disc. The weight of these components is 45.16 kg while the weight of the system to support the heat treatment of these components is 149.18 kg. So, only one fourth of the loaded material is actually to be heat treated. The heating and subsequent cooling of the supporting materials only accounts for heat loss. The loading also depends on the actual volume and height of the loaded components. Since the plates are of small height and larger base, the effective loading of the actual material is decreased. The loading can be as high as 50% for other ceramics products.

5.1.2 Internal and external wall temperature of the furnace

A k-type thermocouple fitted inside the furnace measures the internal temperature of the furnace during its operation while the temperature of the external wall of the furnace is

measured using an infrared thermometer gun. The temperature is measured at various locations of the outer walls and an average value is calculated. Temperature measurement at the beginning is calculated for small intervals while at the later stages the temperature is measured at interval of 1 hour 30 minutes. The total process is completed in 11 hours and 30 minutes, that is, 41,400 seconds. The firing started from 6:15am and completed at 5:45 pm in the evening after reaching the temperature of 1075°C. The furnace has an opening at the front wall which is kept open until the temperature reaches around 200 to 300°C to let the moisture present, if any, to escape. The ambient temperature is considered 25°C at the beginning of the process and convection coefficient for the simplified case of stagnant air is considered.

The data for the external wall temperature, internal temperature of furnace and the loading are as presented below.

Table 5.2: Time-temperature data of the internal and external wall of furnace

Time(s)	Temperature (°C)			
	Internal	**LS wall**	**Front wall**	**Top cover**
0	25	25	25	25
900	78	28.49	27.74	28.94
5400	257	37.7	33.36	34.54
10800	465	48.38	51.91	56.66
16200	618	58.87	70.89	72.23
21600	742	70.578	77.4	89.98
27000	865	82.68	91.13	103.37
32400	954	94.39	101.9	121.19
37800	1027	104.68	108.39	128.88
41400	1075	111.7	114.7	136.64

The measured temperature of the outer wall of furnace above 70°C is higher than that suggested in the literature (Mariños Rosado et al., 2020). So, considerable amount of heat loss taking place from the furnace wall is clear from the temperature data. The minimum temperature is $25°C$ which is at the start of the heat treatment process. The wall temperature reached maximum value of 136.64°C for the top cover. These higher

temperature values are an indication that the factors such as wall material, configuration or the environment is not optimum for the operation of the furnace.

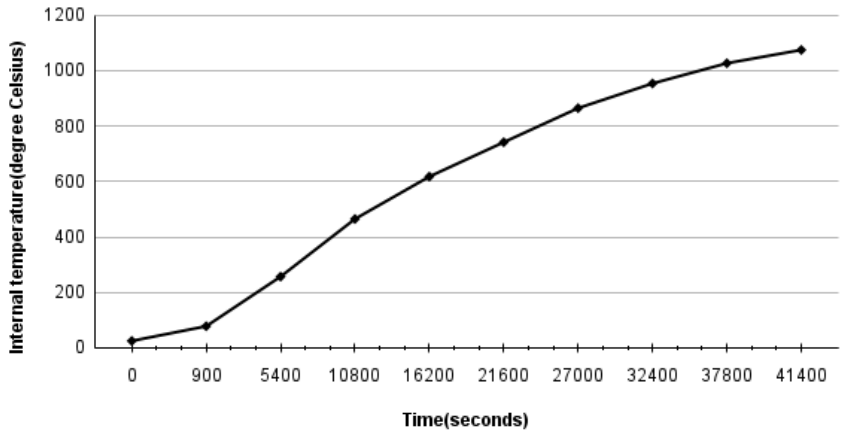

Figure 5.1: Time-temperature graph for the internal wall of furnace

The time-temperature graph for the internal temperature of the furnace is as shown in Figure 5.1. It shows that the temperature rise rate is steeper at the beginning of the process. The slope of the line gradually decreases as the process proceeds towards completion. In the first 900 seconds, the temperature rise rate is $3.53°C/\text{min}$ which decreases up to $0.80°C/\text{min}$ for the final time step.The initial temperature is $25°C$ and the final temperature reached is $1075°C$ when the process completes. The curve is not completely horizontal when the process completes and has a positive slope. So, it can be deducted that the process does not reach a steady state at its completion.

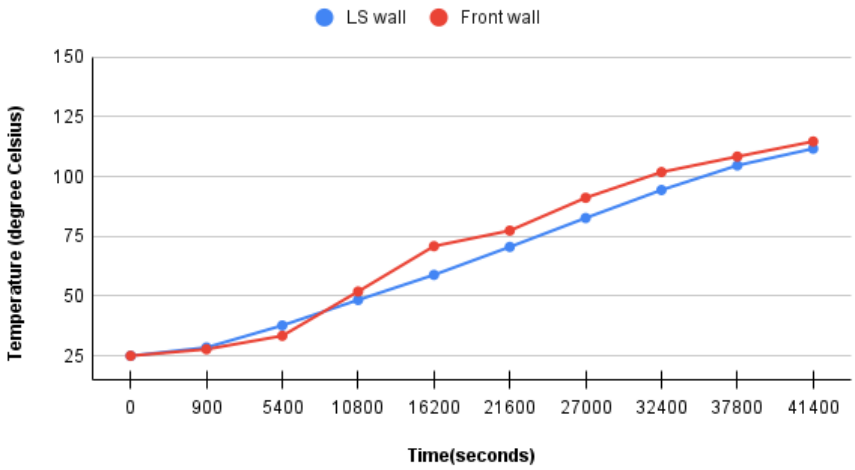

Figure 5.2: Temperature on different outer wall of furnace

The figure 5.2 shows the temperature distribution on the outer wall of the furnace. Initially the wall is at the same temperature as the ambient air temperature of $25°C$. This

temperature rises up to 111.7°C for the lateral walls while the temperature is 114.7°C for the front wall. The higher temperature on the front wall can be attributed to the small exhaust hole present on the furnace front wall which is only closed after the furnace reaches the temperature of around 250°C to let any moisture present, if any, to pass out of the furnace as vapour.

5.1.3 Measuring of the weight of the ceramics after firing

The ceramics product was again weighed after the completion of the firing process.

Table 5.3 Total weight of the ceramics product before and after firing

S. No	Components	Quantity	Weight(kg/piece)	
			Before firing	After firing
1	Big plate	20	1.118	1.089
2	Small plate	20	0.756	0.737
3	Small disc	80	0.096	0.092
Total weight(kg)			45.16	43.88

The difference in the weight of the ceramics is only for the plates and the disc, other materials that help in loading remain the same. The difference in total weight after the heat treatment is only 1.28kg. The difference in weight is the loss of the moisture present in the glazed ceramic material during the heat treatment process.

5.1.4 Measuring the dimensions, current and power

The furnace wall has the external dimensions of $1280 \times 1000 \times 820$mm. Hence, the total surface area of the external wall of the furnace is calculated to be 3.7392m^2.

The diameter of the wire used is 1.7mm and it is coiled to form a helix of diameter 25.4mm. The number of turns are counted for a certain length of the wire to find the pitch of the coil and the straight wire length of the wire is obtained using the following relations.

$$L = n\sqrt{c^2 + p^2} \qquad \textit{Equation 5.1}$$

Where L is the length of the wire, n, c and p are the number of turns, circumference of helix and the pitch of the wire.

$$n = \frac{H}{p} \qquad \textit{Equation 5.2}$$

Where H is the total length of the helix

$$c = \pi . d \qquad \textit{Equation 5.3}$$

The straight length of the coil is calculated to be 207 metres from above equations for the coiled wire length of 18.72 metres with pitch of 7mm.

The surface area of the wire is calculated using the following relation.

$$A_s = 2\pi rL \qquad \textit{Equation 5.4}$$

$$A_s = 2\pi(0.85 \times 10^{-3})(207) = 1.105\ m^2$$

A digital clamp meter is used to measure the current passing through the wires which is 52.5 Amperes at the beginning of the heating process and the supply voltage is 220 Volts.

5.1.5 Energy input calculations

The heating element is assumed to have 100% emitting efficiency. Hence, the rated power of the electric resistance furnace is,

$$\text{Power(P)} = 11.5\ \text{kWh}$$

Electricity consumed during the operation of furnace for 11.5 hours is

$$\text{Total electrical energy consumed} = \text{Power(P)} \times \text{time(t)} \qquad \textit{Equation 5.5}$$

$$= 11.5 \times 11.5 = 132.25\ \text{units}$$

There was no individual sub-meter installed for each of the electric resistance furnace and multiple furnace were in operation at the same time. So, the energy consumed is calculated using the relation 5.5.

5.1.6 Temperature of heating coil

It is suggested from the literature that the temperature measured by the thermocouple can be off by as much as 100℃ according to the placement of the thermocouple (C. Barry Carter, 1974). Since the thermocouple is not placed on the wall very close to the heating element, its temperature is taken to be $1300°C$ which is the maximum continuous operating temperature of the Kanthal A wire.

Figure 3.3: Furnace wall with the Kanthal wire and thermocouple

This temperature is confirmed by calculating the temperature for the Kanthal wire from the handbook(*Heating Element Design Factors*). The diameter of the wire used is 1.7 mm which has a resistance of 0.612Ω/m at $20°C$. The surface area and the weight of the wire are taken from the handbook. The temperature of the heating element can be calculate from the following relation with the resistance value measured at start of the process and process completion.

$$R_2 = R_1[1 + \alpha_s(T_2 - T_1)] \qquad \textit{Equation 5.6}$$

5.2 Computational results

The model of the furnace wall, furnace wall with domain and with an object placed at the centre are each subjected to computational study in ANSYS Transient Thermal.

5.2.1 Transient thermal analysis of the walls

The total process of the heat treatment completes in 11.5 hours. So, it is not be possible to simulate the whole process with each and every seconds considered. So, the analysis is done by taking certain time steps. The time dependent solver is used to obtain the solution for the model from 0 to 41400 seconds by taking 10 steps with an initial step of 900 seconds and then every step of 5400 seconds. Each of these 9 steps were divided into 180 sub steps with a single sub-step of 30 seconds. After defining the time step, other boundary conditions were applied and the analysis is carried out.

The outer wall temperature and heat flux at different time intervals of the transient thermal analysis for the model with walls are as shown in the plots below.

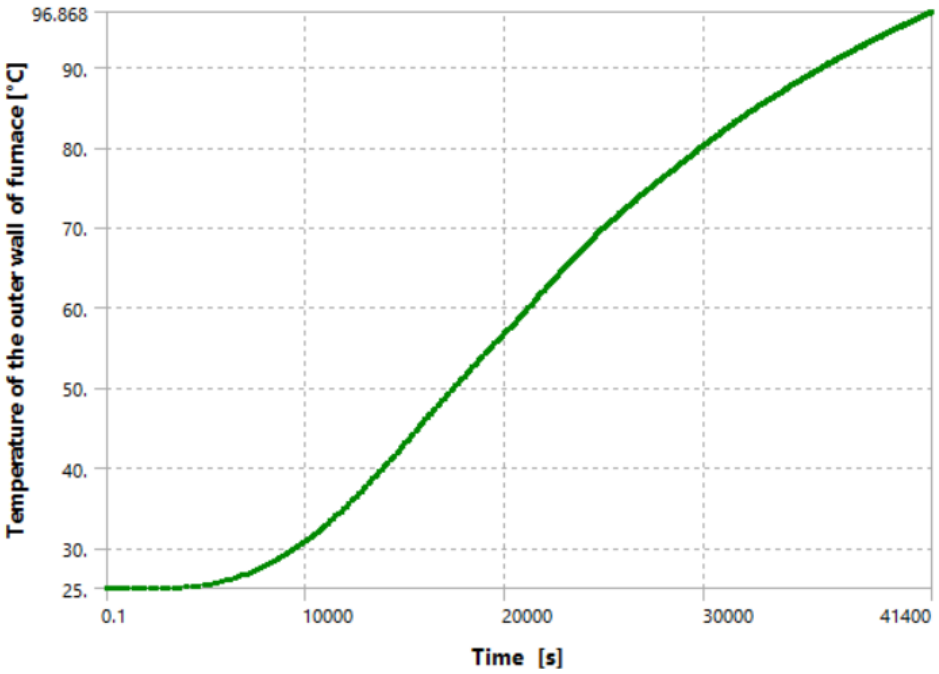

Figure 5.1: Transient temperature vs time plot for outer wall of furnace

The initial condition of the heating process starts from room temperature of $25°C$. The minimum temperature is at the beginning and the maximum temperature is at the end of the process. The temperature of the outer wall rises steadily to $96.86°C$ when the heating process completes at 11.5 hours or 41,400 seconds.

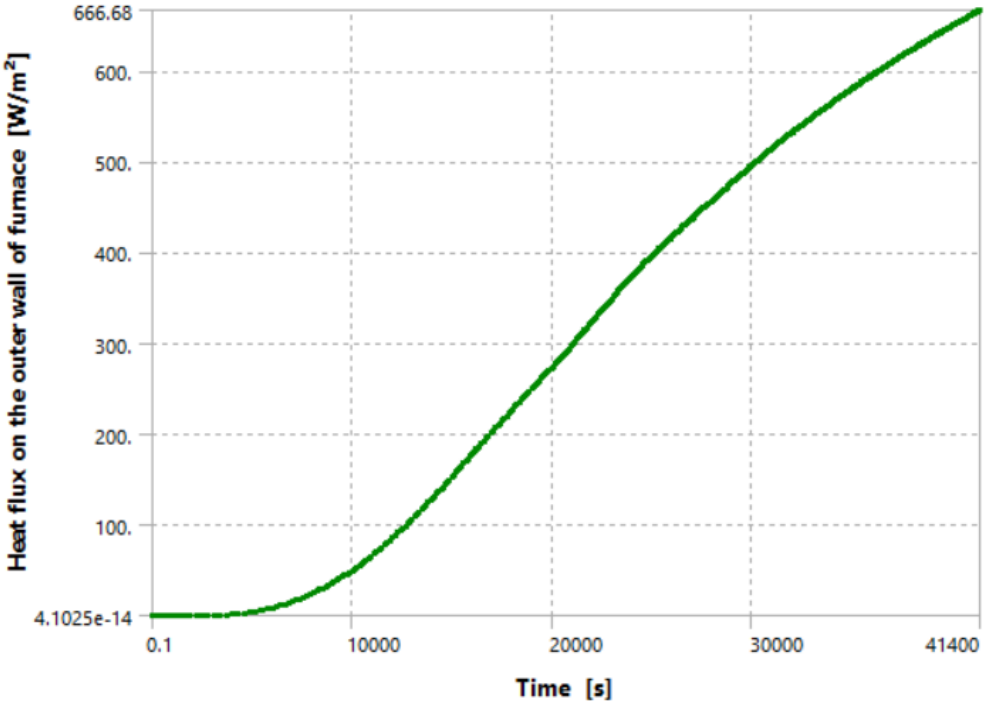

Figure 5.2: Transient heat flux vs time plot for outer wall of furnace

The heat flux through the wall is almost zero at the beginning of the furnace operation which rises steadily to a value of 666.68 Wm^{-2} after 41,400 seconds as the process completes. This is the maximum value for heat flux passing out through the walls.

The temperature contour and isotherms for the whole wall layer and the outer wall are as presented in the figures below.

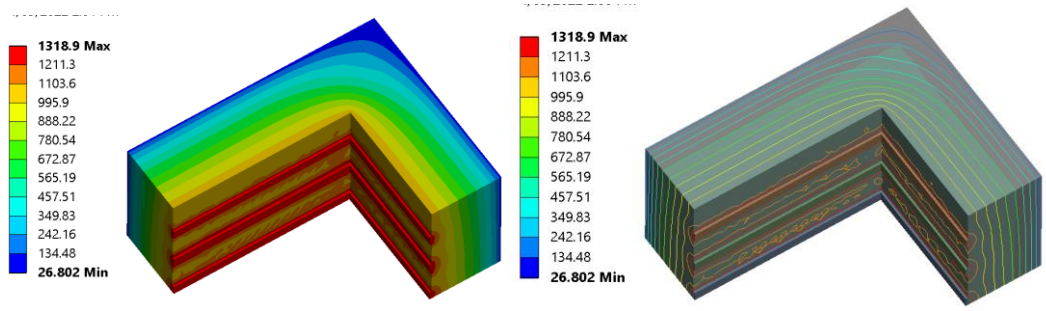

Figure 5.3: Temperature contour and isotherms for the wall

From the temperature contour, it can be seen that the corner of the L-shaped wall has the minimum temperature of 26.80°C while the heating element at the centre has the highest temperature of 1318.9°C. Hence the temperature distribution is not uniform through the wall. Also very low heat passes through the corner of these furnace walls indicating that the temperature rise is minimum there. This is due to the radial distance of the outer corner of the wall being at the farthest distance from the heating element present inside the furnace.

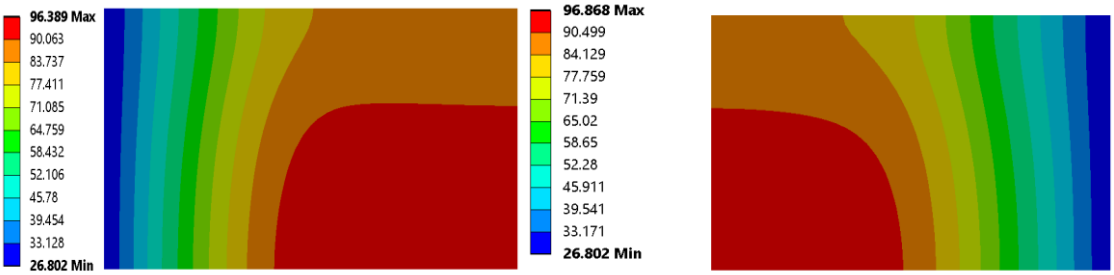

Figure 5.4: Temperature contour on (i) longer and (ii) shorter sides of L-shaped wall

The temperature contour shows that the minimum temperature of 26.802°C is same for both the walls. The maximum outer wall temperature for the shorter side of the wall is 96.86°C while the maximum outer temperature for the longer side of the wall is 96.38°C which is slightly lower than that for the shorter side of the wall. Towards the middle section of the outer wall, the temperature and hence the heat flux passing per unit area is more than at other section of the furnace wall.

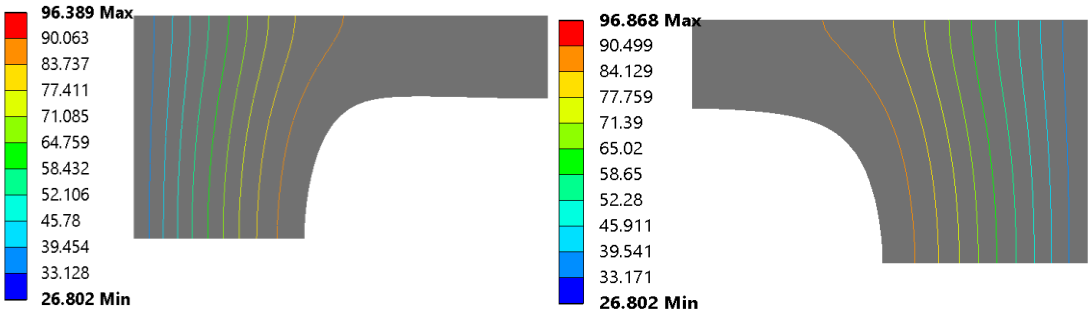

Figure 5.5: Isotherms for the outer surface of the longer and shorter side of the wall

Similarly the isotherms for the longer and shorter side of the wall are similar. The isotherms are almost straight at the corner wall of furnace while it is almost a 90° bend at the middle section of the wall.

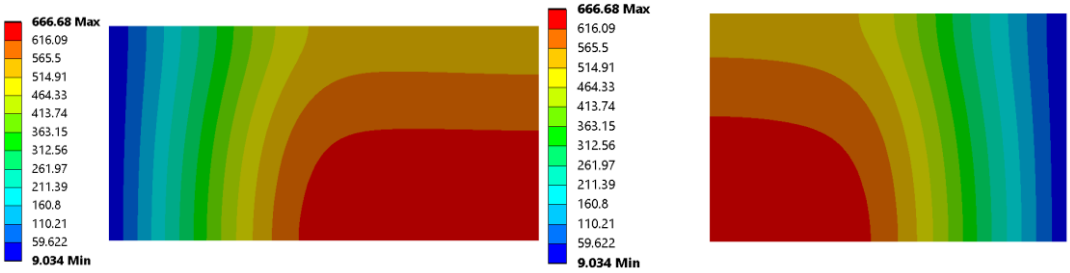

Figure 5.6: Heat flux contour on (i) longer and (ii) shorter sides of L-shaped wall

The heat flux contour on both the sides of the wall show the same maximum and minimum value because both the faces of the wall share a common edge.

5.2.2 Transient thermal analysis of model with air domain

The temperature contour and isotherms for the model with the air domain are as presented in the figures below.

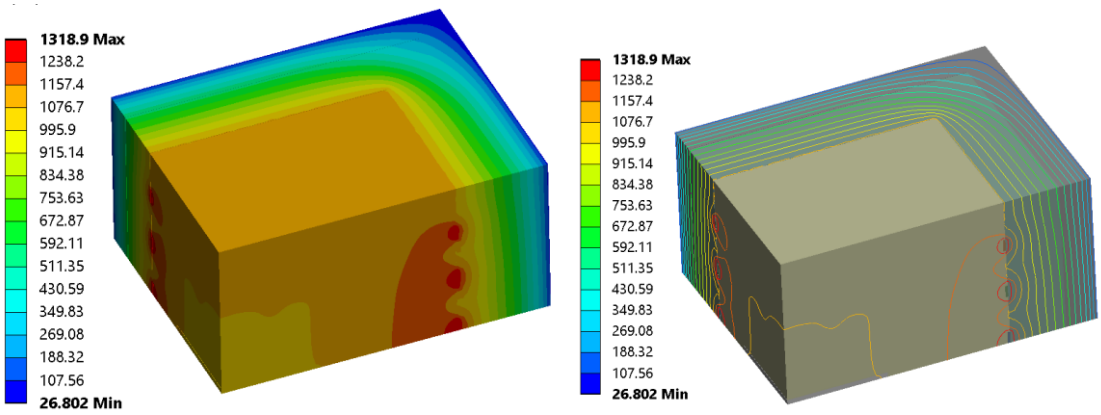

Figure 5.7: (i) Temperature contour and (ii) isotherms for model with air domain

The temperature contour suggests that the temperature at the region near the heating element is the maximum which is 1318.9°C while the minimum temperature is on the

corner of the L-shaped wall. Also, the temperature is gradually decreasing towards the centre of the furnace as the distance from the heating element increases. There is a region of lower temperature in the middle than at the other areas of the domain.

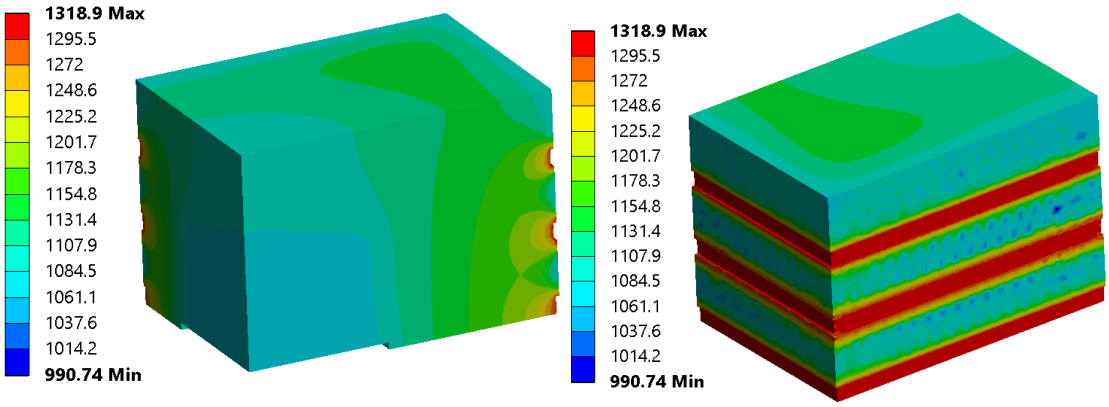

Figure 5.8: Temperature contour on the air domain

The minimum temperature of the air domain is 990.74°C while the maximum temperature is 1318.9°C. Hence, the average temperature of the air domain inside the furnace is 1132.6°C. The minimum temperature occurs on the central region of the air domain while the maximum temperature occurs on the region next to the heating element. The heated air gets distributed and the last to be heated is the central region of the furnace.

In the analysis of this model with the air domain, the temperature distribution on the air domain were studied by creating planes passing through the symmetry surface and centre of the domain.

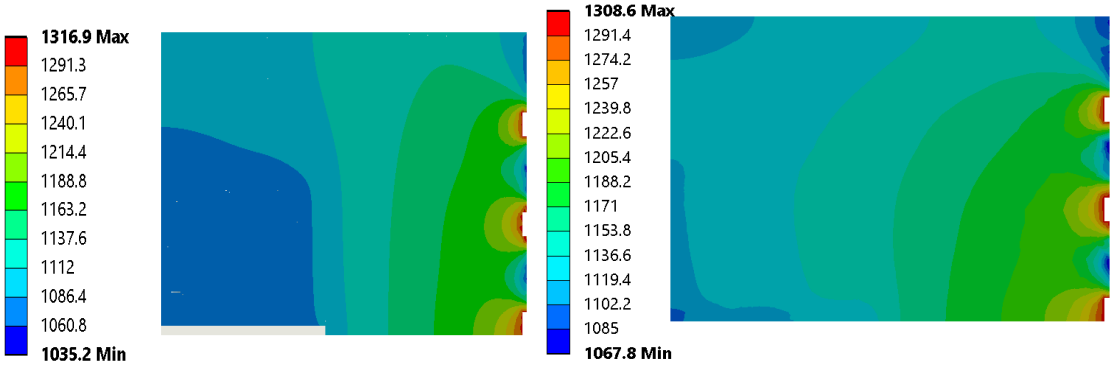

Figure 5.9: Temperature distribution on the air domain (i) through the symmetry surface of model (ii) through the centre of the domain

The maximum temperature on the symmetry surface of the domain is 1316.9°C. On the plane passing through the centre of the domain, the maximum temperature is 1308.6°C and it occurs at the heating element. The minimum temperature on the surface of the domain is 1035.2°C while the minimum temperature on the plane passing through the

centre of the domain is 1067.8°C. This result suggests that the temperature on the air domain is not symmetrical and vary from point to point. Though the temperature of the air is higher around the heating element, this heat ultimately flows in the whole chamber and the heat flows towards the centre of the chamber from the wall side and the centre portion of the furnace is the last to be heated.

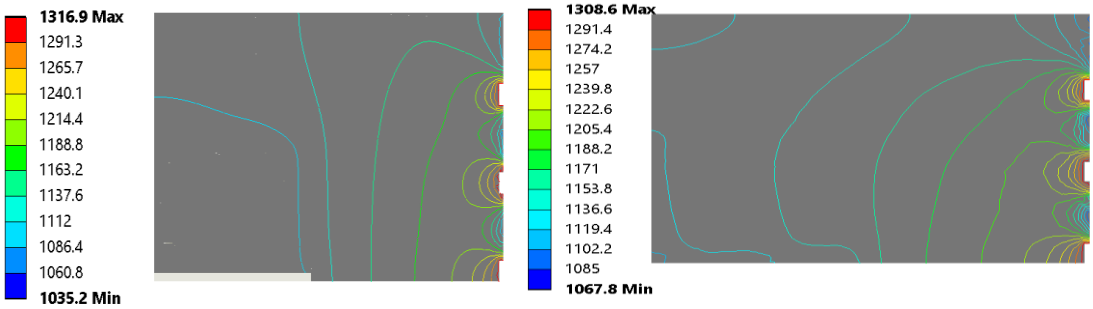

Figure 5.10: Isotherms on the (i) symmetry surface (ii) surface passing through centre of the air domain

The isotherms are nearly semicircular near the heating element in both the planes. These isotherms are not uniform and hence are shaped and spaced unevenly. These isotherms end at right angle to the edge of the domain.

5.2.3 Transient thermal analysis with load or centrally placed object

In the analysis of this model, the temperature distribution and heat flux distribution were analysed for the walls, object and the air domain inside. The temperature distribution and the corresponding isotherms on the walls, domain as well as the object are shown in the figures below.

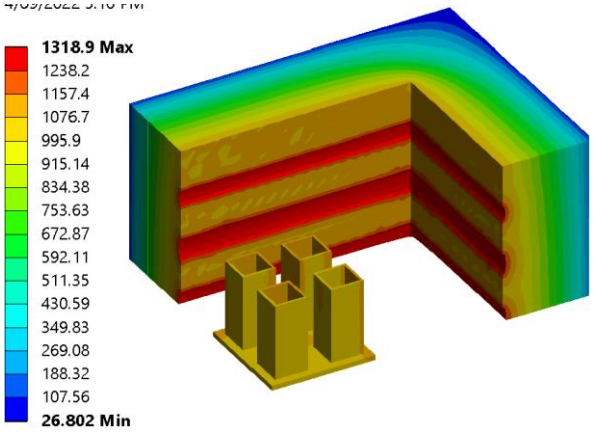

Figure 5.11: Temperature contour on computational domain

The minimum temperature of the whole computational domain is on the outer corner of furnace wall which is equal to 26.80°C while the maximum is on the heating element, it

is equal to 1318.9°C. The temperature distribution on the object is seen more or less uniform compared to the total domain of study.

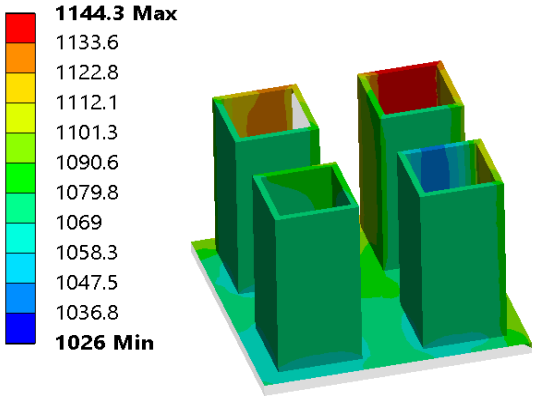

Figure 5.12: Temperature contour on the central object

From the figure 5.13, we can observe that the maximum temperature of the object is 1144.3°C while the minimum temperature is 1026°C. Hence, the average temperature of the object is 1087.2°C. This temperature is sufficient for the sintering process of the ceramics. The higher temperature is on the side of the object which faces the heating elements. Hence, it can be concluded that the objects exposed directly to the heating elements are raise to more temperature while for the other faces the temperature is uniform to a certain degree.

5.3 Comparative analysis

The data obtained from the computational and experimental study need to be analysed. A comparative analysis of the external temperature and internal temperature of the furnace is carried out.

5.3.1 Outer wall temperature of the furnace

Considering the symmetry of the furnace, computational study was carried out by creating the model for one-eighth part of the wall and subjecting it to study in ANSYS Transient Thermal. Experimental data for the temperature of outer wall of furnace was collected from the field visit at Sanothimi. The computational and experimental value have a certain difference in the values of the external temperature of the wall of the furnace as plotted in the graph below.

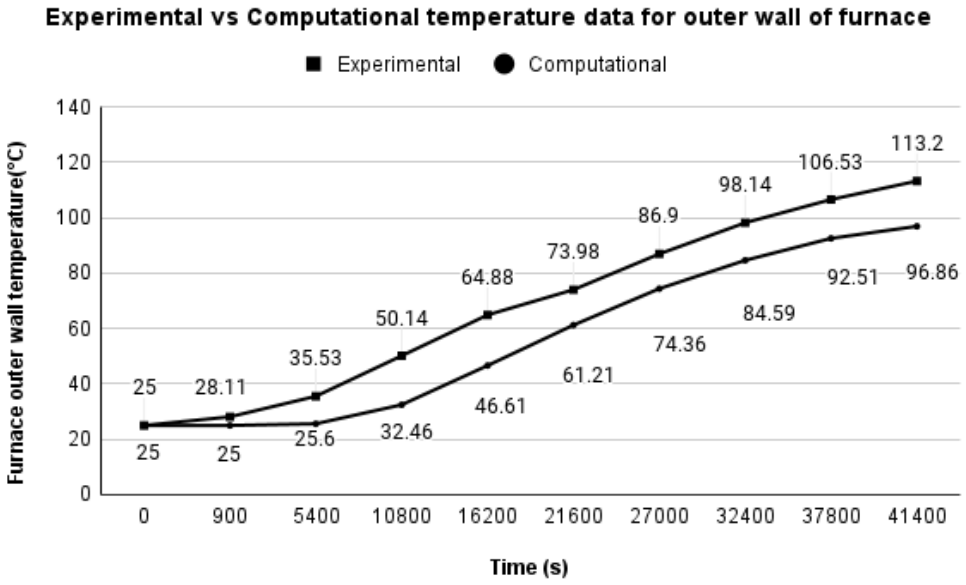

Figure 5.13: Comparison of experimental and computational temperature of the furnace outer wall

The trend of the average of the experimental values of the temperature is same as the computational values but they are higher than the computational values. The final experimental value of the temperature of 113.2°C is higher by 16.33°C than the computational value of 96.86°C. The suggested outer wall temperature from the literature should lie between 60 to 70°C(Mariños Rosado et al., 2020). This shows that either the insulation is insufficient or the walls have some unaccounted defects that allow for the heat leakage from the system. A contributing factor can be the cementing material for the walls, which is not taken into account in this study. Another possible reason could be due to lack of periodic maintenance of the furnace.

From observation during experimental data collection, the outer insulation layer was seen torn in certain places and protruding out from the casing. Also, cracks were seen in the refractory bricks when the inside of the furnace was observed. Moreover, the white paint inside the furnace was not uniform, clearly indicating that the furnace lacks periodic maintenance. The inner wall of the furnace needs to be coated with high emissivity coatings such as white heat-K that allows the heat produced inside the furnace to remain inside the furnace.

5.3.2 Inner wall temperature of the furnace

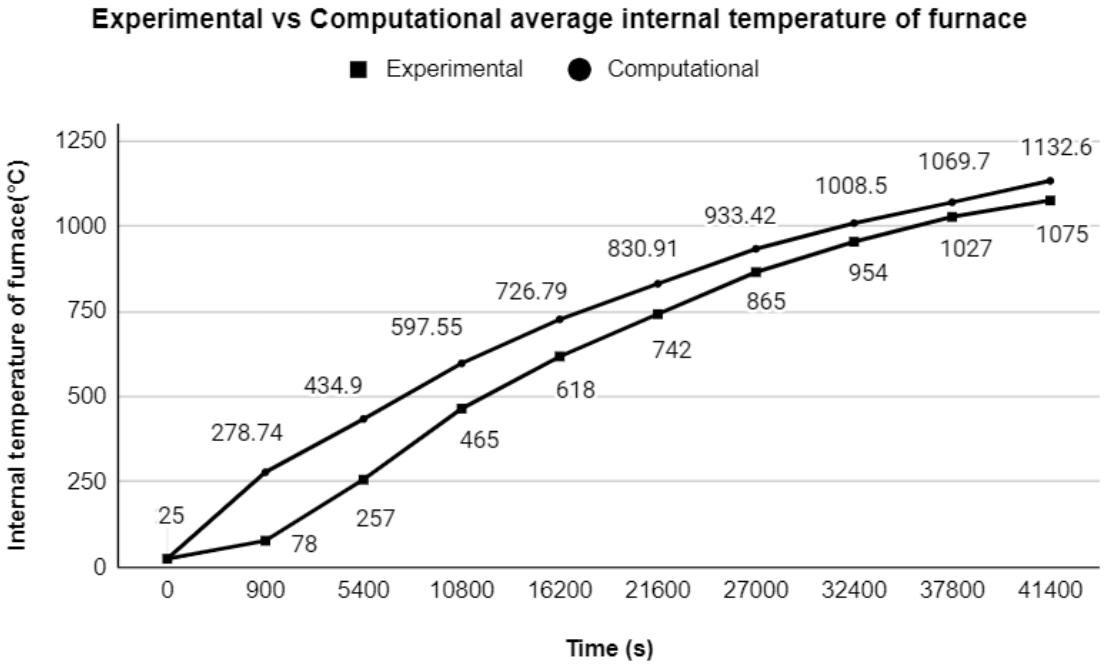

Figure 5.14: Comparison of experimental and computational internal temperature of the furnace

The average temperature of the internal furnace environment obtained from the computation is 1132.6 $°C$ at the process completion which is higher by 57.6$°C$ than the experimental value of 1075$°C$. This is a deviation by around 5.35% from the experimental value. Although the starting temperature is 25$°C$, the gap between the two curves is large in the first few time intervals. As the process proceeds, the temperature gap eventually decreases between the two curves.

5.3.3 Energy loss and efficiency calculations

Applying energy balance to the furnace, the energy supplied through the coils is majorly utilized in heating the air, ceramic materials loaded inside the furnace and heating the walls of the furnace.

Total energy supplied,

$(\mathrm{Q}) = P.t = 476.1MJ = 132.25\ units$

Inside the furnace, the amount of heat absorbed by the ceramic materials is the only useful heat put into work. Taking the specific heat of ceramic material to be 1200 J/kgK, and the average temperature of the ceramic at the end of the process is obtained to be 1087.2$°C$

Total heat energy absorbed by ceramic materials,

$(\mathrm{Q_c}) = m_c C_{pc} dT = 193.06 \times 1200 \times 1050 = 244.87MJ$

Total heat energy absorbed by air,

$(\mathrm{Q_a}) = m_a C_{pa} dT = 0.4472 \times 1006.4 \times 1100 = 495.408kJ$

Total heat energy absorbed by moisture,

$(\mathrm{Q_m}) = m_m C_{pm} dT + m_m L_v = 1.28 \times 4200 \times 100 + 1.28 \times 2.25 \times 10^6 = 3.417\ MJ$

The average temperature of the refractory wall is 836.58°C and the average temperature of the insulation layer is 322.97°C.

Average heat energy stored in the refractory wall

$(\mathrm{Q_r}) = m_{rw} C_{rw} dT = 217.416 \times 880 \times 811.58 = 155.25MJ$

Average heat energy stored in the insulation

$(\mathrm{Q_i}) = m_{iw} C_{iw} dT = 34.34 \times 1070 \times 297.97 = 10.94MJ$

Total heat energy utilized

$(\mathrm{Q_T}) = 244.87 + 0.495 + 3.417 + 155.25 + 10.94 = 414.972\ MJ$

Therefore, the loss of heat energy through the outer wall of furnace and other unaccounted losses due to efficiency of heating coil, heat energy stored in the heating coil, overheating of the ceramics that directly faces the heating coil is equal to

$(Q_L) = Q - Q_T = 476.1 - 414.972 = 61.128\ MJ$

The percentage of heat energy loss is given as,

$$\text{Loss of heat energy} = \frac{Q_L}{Q} = \frac{61.128}{476.1} = 12.83\%$$

The actual thermal efficiency of the furnace in the heat treatment of ceramics is the ratio of heat energy absorbed by the ceramic material to the total heat energy supplied by coil.

$$Efficiency(\eta_c) = \frac{\text{Heat energy utilized}(\mathrm{mC_p dT})}{\text{Heat energy supplied}(P.t)} = \frac{244.87}{476.1} = 51.4\%$$

As obtained from simulation, the internal temperature reaches a value of 1075.1°C at 37,860 seconds or 10.516 hrs, the thermal efficiency then becomes

$$Efficiency(\eta'_c) = \frac{\text{Heat energy utilized}(\mathrm{m_c C_{pc} dT})}{\text{Heat energy supplied}(P.t)} = 54.04\%$$

5.4 Further analysis of the walls

The wall of the existing wall is 180mm thick with the high alumina refractory brick of 115mm and insulation of 65mm. The temperature distribution on the wall and the external temperature is a matter of interest. The heat supplied by the heating element is dissipated by conduction through the walls, convection through the air inside the furnace and radiation to heat the load inside the furnace. Taking the furnace to be a closed enclosure,

the conduction through the walls is the main way of heat dissipation from the whole furnace.

5.4.1 Analysis from computation in ANSYS

The temperature distribution on the walls of the furnace along a straight line starting from just behind the heating element to the furnace outer wall as obtained from the computation in ANSYS at the end of 11.5 hours or process completion is as shown in the Figure 5.15.

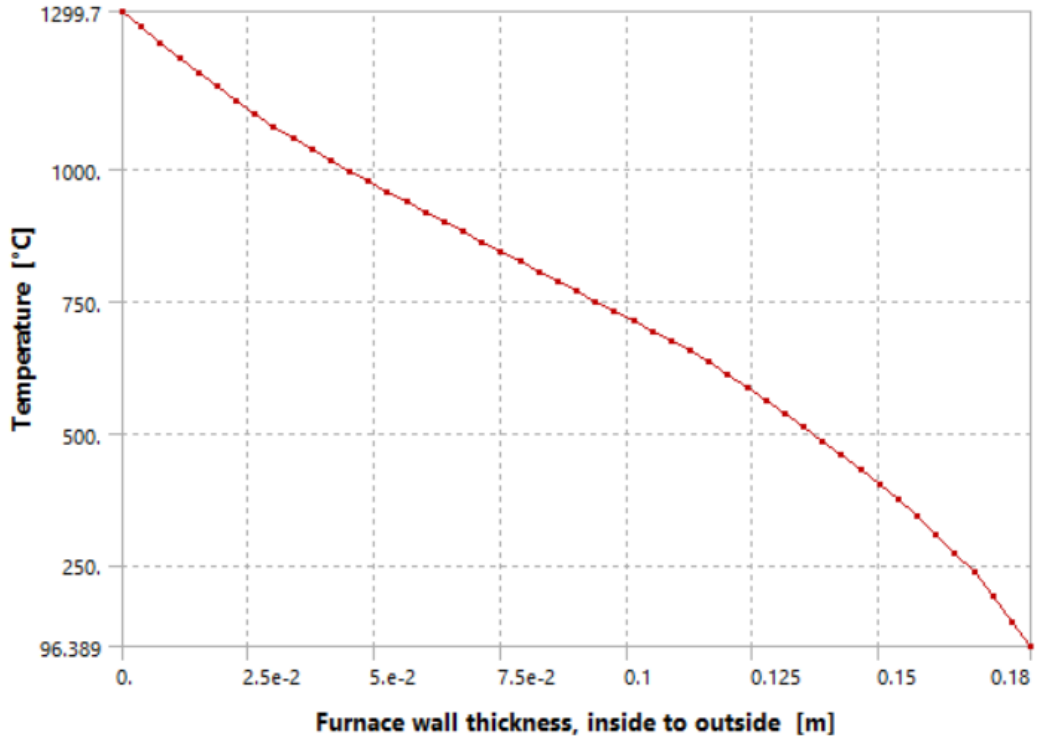

Figure 5.15: Temperature distribution along the thickness of the wall

It can be observed that the slope of the temperature variation curve along the thickness of the wall falls steeply as we move towards the outside of the wall. The temperature falls almost linearly through the refractory wall layer. The slope of the line falls more steeply after the 115mm thickness of the wall, that is, when the insulation layer is encountered.

5.4.2 Analysis of conduction through the furnace wall in MATLAB

The thermodynamic properties; density(ρ), thermal conductivity(k) and specific heat capacity(c) play a role in the heat transfer phenomena.

$$\frac{\partial}{\partial x}\left(k\frac{\partial T}{\partial x}\right)+S=\rho c\frac{\partial T}{\partial t} \qquad \textit{Equation 5.7}$$

These quantities vary with temperature but for analysis in the MATLAB, the average value of these properties are taken for both the refractory wall and insulation layer materials.

Table 5.4: Average value of the thermodynamic properties

Thermodynamic properties	**Units**	**Materials**	
		Refractory brick	**Ceramic fibre blanket**
Thermal conductivity	J/(kg K)	0.17	0.078
Density	kg/m³	550	128
Heat capacity	W/(m K)	880	1070

Then the weighted average of these two materials is calculated for each of the three properties and one dimensional transient heat conduction study is performed by applying the boundary conditions.

Weighted average values:

Thermal conductivity$(k) = \frac{0.115\times0.17+0.065\times0.078}{0.115+0.065} = 0.11143 J/(kgK)$

Density $(\rho) = \frac{0.115\times550+0.065\times128}{0.115+0.065} = 397.611 kg/m^3$

Specific heat capacity$(c) = \frac{0.115\times880+0.065\times1070}{0.115+0.065} = 948.611 kg/m^3$

The MATLAB code is based on the finite volume method. Integrating the terms on the right of equation 5.7 we get,

$$\int_{t^0}^{t^1}\int_0^1\int_0^1\int_w^e \left(\rho c\frac{\partial T}{\partial t}\right) dxdydzdt = (1\times1)\Delta x\rho\int_{t^0}^{t^1}(c\frac{\partial T}{\partial t})\,dt \qquad \textit{Equation 5.8}$$

Similarly, integration of the term on the left gives

$$\int_{t^0}^{t^1}\int_0^1\int_0^1\int_w^e \left(\frac{\partial}{\partial x}\left(k\frac{\partial T}{\partial x}\right)\right) dxdydzdt = (1\times1)\int_{t^0}^{t^1}\left[\left(k\frac{\partial T}{\partial x}\right)_e - \left(k\frac{\partial T}{\partial x}\right)_w\right] dt \quad \textit{Equation 5.9}$$

Introducing the weighing factor (f), collecting the terms and dropping the superscript for convenience, we get

$$a_P T_p = a_E f T_E + a_E^0(1-f)T_E^0 + a_w f T_w + a_w^0(1-f)T_w^0 + \left[a_p^0 - (1-f)a_E^0 - (1-f)a_w^0\right]T_p^0 \qquad \textit{Equation 5.10}$$

Where, $a_E = \frac{k_e(1\times1)}{(\delta x)_e}, a_E^0 = \frac{k_e^0(1\times1)}{(\delta x)_e}$

$a_w = \frac{k_w(1\times1)}{(\delta x)_w}, a_w^0 = \frac{k_w^0(1\times1)}{(\delta x)_w}$

$a_P^0 = \frac{\rho\bar{c}\Delta x(1\times1)}{\Delta t}, a_P = f a_E + f a_w + a_P^0$

For explicit scheme f=0, for implicit scheme, f=1 and for Crank Nicholson scheme, f=1/2 is replaced in the equation 5.9. The result obtained from three different schemes is as shown in figure 5.16 below.

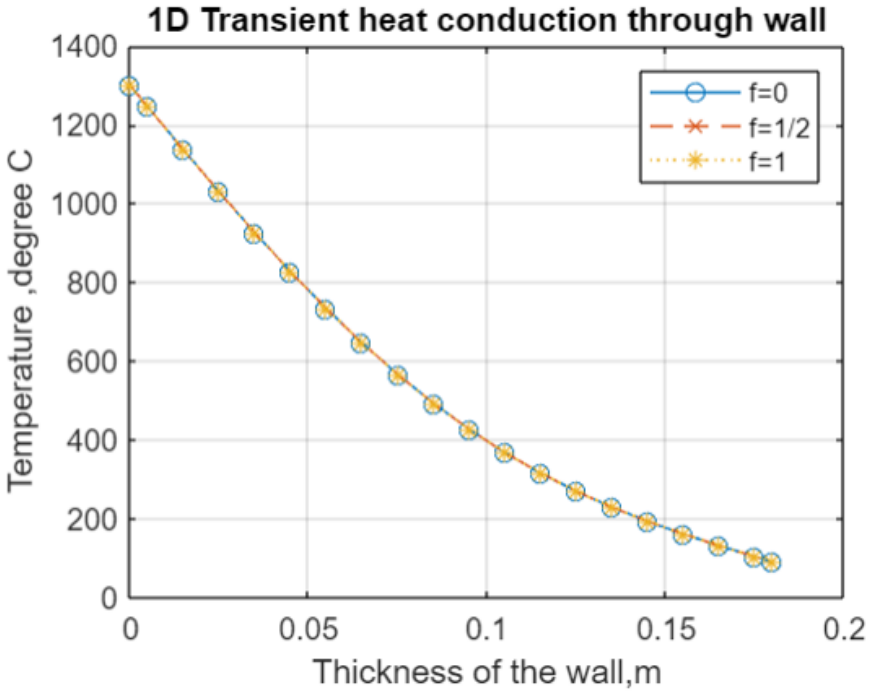

Figure 5.16: Temperature variation on furnace wall through different schemes

The result from three different schemes; implicit, explicit and Crank-Nicholson scheme are almost identical. The temperature on the outer wall is obtained to be 90.28°C.

As compared to the result obtained from computation in ANSYS, this temperature of 90.28°C is lower by around 6°C. This variation might be because of the fact that the study carried out in MATLAB is one dimensional and the average value for the thermodynamic properties of the substances are taken. Because of this reason, the analysis in MATLAB does not depict the actual temperature distribution on the furnace wall. The nature of the two curves are quite different except for at the beginning. The analysis in MATLAB just shows that the outer skin temperature of the furnace wall is well in the range as obtained from the analysis in ANSYS.

5.5 Alterations in the wall

The value of temperature on the outer wall of furnace is high as compared to the industrial standards which suggest the wall temperature to be between 60 and 70°C (Mariños Rosado et al., 2020). So, a detail analysis of the furnace wall materials and thickness can be carried out in an attempt to reduce the outer wall temperature and hence the heat loss through the outer walls of furnace. Since, refractory bricks are produced in standard dimensions, while the ceramic fibre blankets come in rolls of different thickness, the only variation of thickness of existing wall can be achieved by varying the thickness of the

insulation. Two different approaches are made in an attempt to reduce the heat loss from outer surface of the walls.

5.5.1 Constant total thickness approach

The first approach is constant total thickness approach in which the total 18cm thickness of wall is kept constant. The standard size of the refractory brick is 115mm, hence the variation can only be made on the insulation layer for the constant thickness. A 20mm thickness of ceramic fibre blanket replacement by different insulation materials and air gap combination is studied. Thermal mass values were calculated for five different insulation materials with working temperature not exceeding maximum temperature of safe use.

Table 5.5: Thermodynamic properties of the different insulating materials

Thermodynamic properties		**Insulating materials**				
	Unit	**Silica**	**Clay**	**Diatomite solid**	**Diatomite porous**	**Alumina**
Thermal conductivity	J/(kg K)	0.40	0.30	0.25	0.14	0.17
Density	kg/m³	830	560	1090	540	910
Heat capacity at constant pressure	W/(m K)	970	878	1308	1250	880
Thermal mass per unit volume	J/(K. m^3)	805100	491680	1425720	675000	800800

Combination of 10mm of each of the five insulating materials were tried with air gap of 10mm and simulations were done. From among these five materials, clay is the one with smallest thermal mass and it is available locally and is cost effective as well. 10mm of clay adjacent to refractory brick and a 10mm of air gap maintained between the clay and ceramic fibre blanket insulation is found to reduce the temperature as well as heat flux on the outer wall of the furnace by a considerable amount than other combinations. The lower thermal mass, easier moldability and easy availability makes clay worth using as an insulating material. Lower thermal mass of clay ensures less heat storage in the walls and hence will not affect the cooling rate of the furnace after the heat treatment process. Also, it is difficult to maintain air gap of more than 1cm without the rigid wall on the outer side of the air gap as convection and air circulation are introduced and this needs further

analysis. The temperature variation along this combination of wall as obtained from the computation in ANSYS Transient Thermal is shown in Figure 5.18.

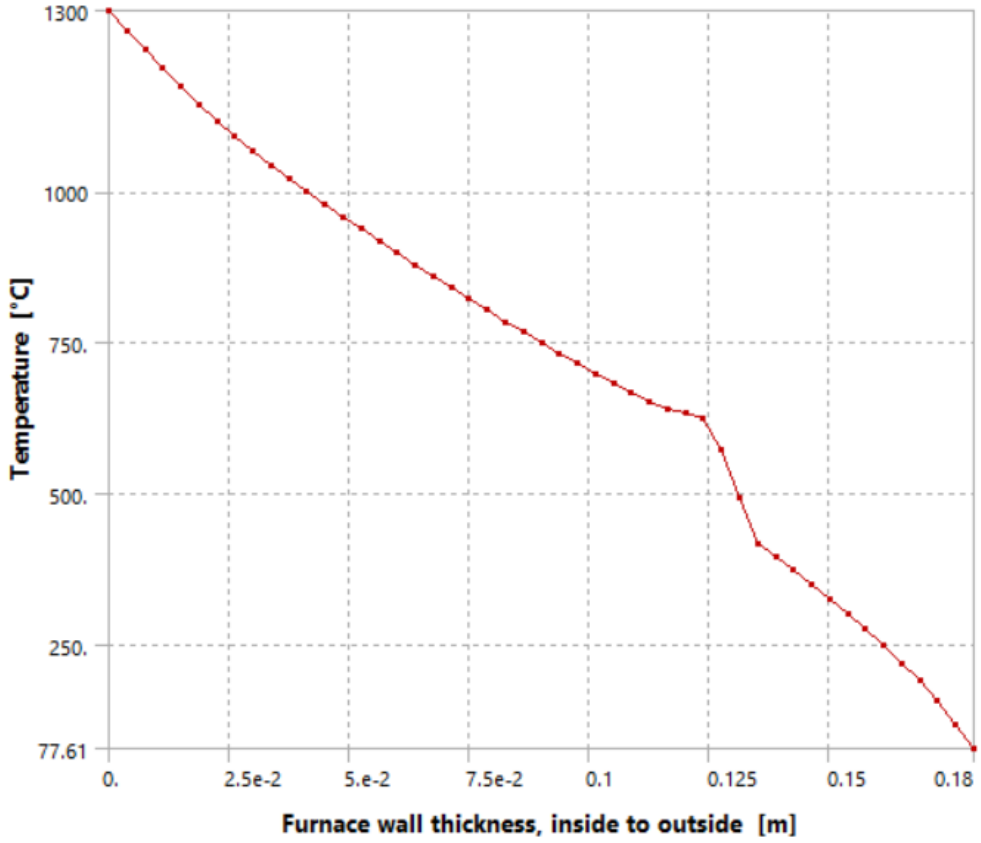

Figure 5.17: Temperature variation on the wall of the furnace with 10mm clay and 10mm air gap

It can be clearly seen from the graph that there is a sharp fall in the temperature after the length of 115mm where a combination of 10mm clay and 10mm air gap is introduced in place of the ceramic fibre blanket. This decreases the minimum temperature reached at the outer wall to $77.608°C$ which is a decrease of $18.78°C$ than the outside wall temperature of the existing wall. This approach can be the low cost method during the reconstruction of the worn out furnaces to reduce the heat loss through the outer wall of the furnace. This also ensures that while focusing on decreasing the outside wall temperature of furnace, the extra heat is not stored in the layers of the wall of the furnace.

5.5.2 Variable total thickness approach

The second approach is variable thickness approach in which the thickness of existing insulation was increased until the maximum temperature on the outer wall falls to $70°C$. A ball park value was obtained from the one dimensional transient thermal analysis by numerical approach and repeated hit and trial simulations were carried out to obtain the

value of 70°C by altering the thickness. With the addition of extra 4cm layer of ceramic fibre blanket on the existing furnace wall, the outside wall temperature of the furnace is reduced to 70. 23°C.

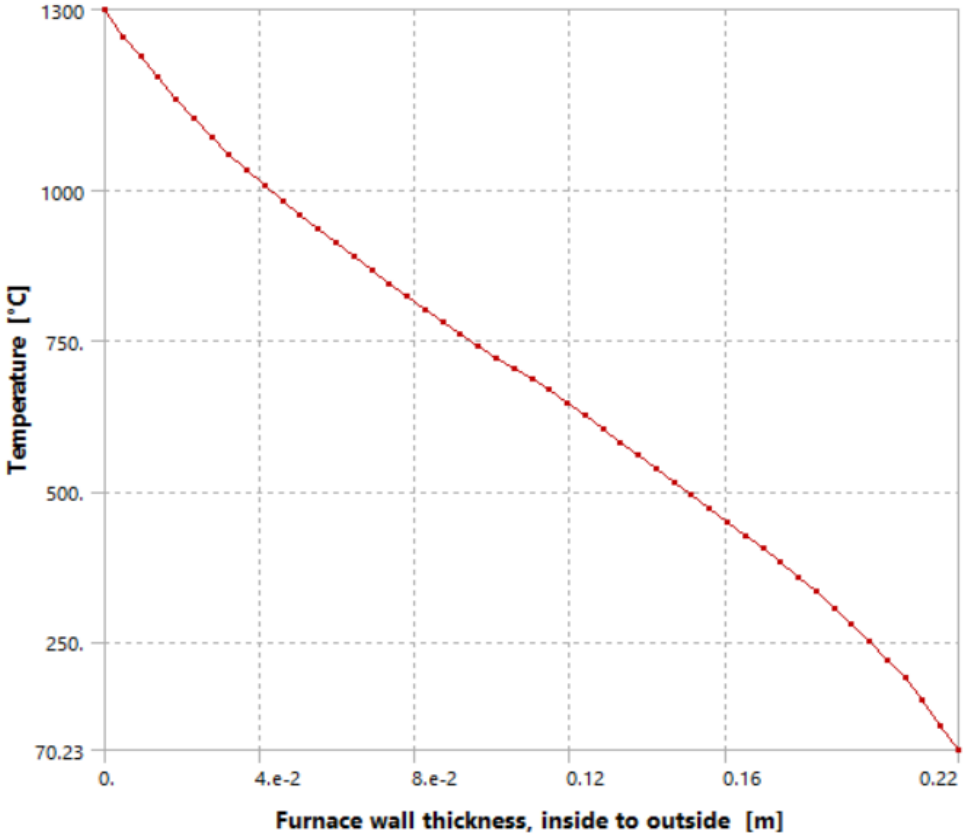

Figure 5.18: Temperature variation on the wall of the furnace with an added layer of 40mm of insulation

The comparison of the maximum outer wall temperature for the existing furnace, wall with an added 4cm thick ceramic fibre insulation and the constant total thickness wall with 10mm of clay and 10mm of air gap maintained adjacent to the refractory brick are shown in the Figure 5.19.

5.5.3 Comparative study of wall variations

The results suggest that the maximum outer wall temperature can be decreased from 96.86°C to 77.61°C with the clay and air gap at the middle of the furnace. Similarly, the maximum outer wall temperature is reduced to 70.23°C from 96.86°C by adding a 40mm layer of insulation outside of the existing wall of furnace.

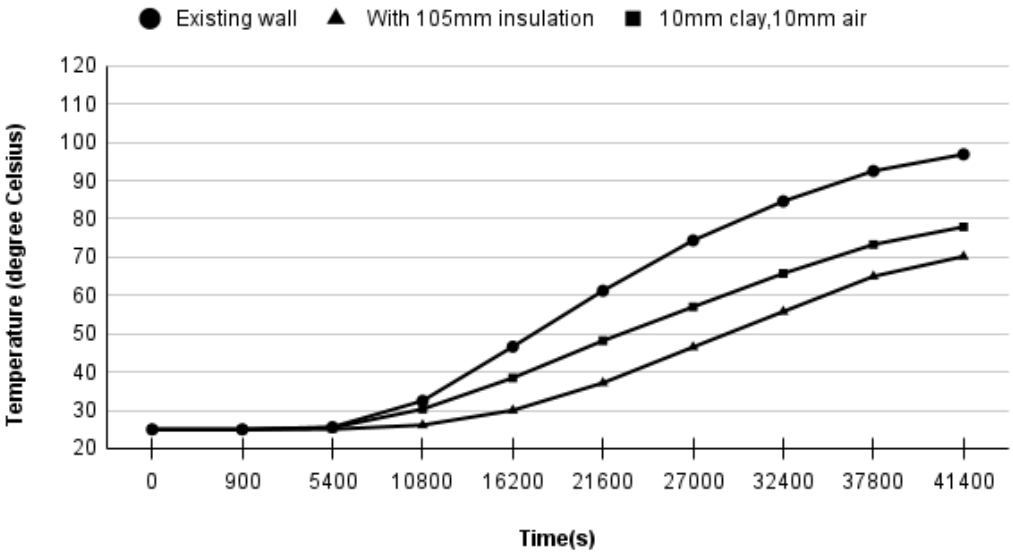

Figure 5.19: Comparison of outer wall temperature at different times for the three models of wall

The heat flux value also suggests the same result. The maximum heat flux passing out of the wall of existing furnace wall is 666.68W/m^2 which can be reduced to 470.67 W/m2 for the combination of clay and air gap adjacent to refractory brick for constant wall thickness.

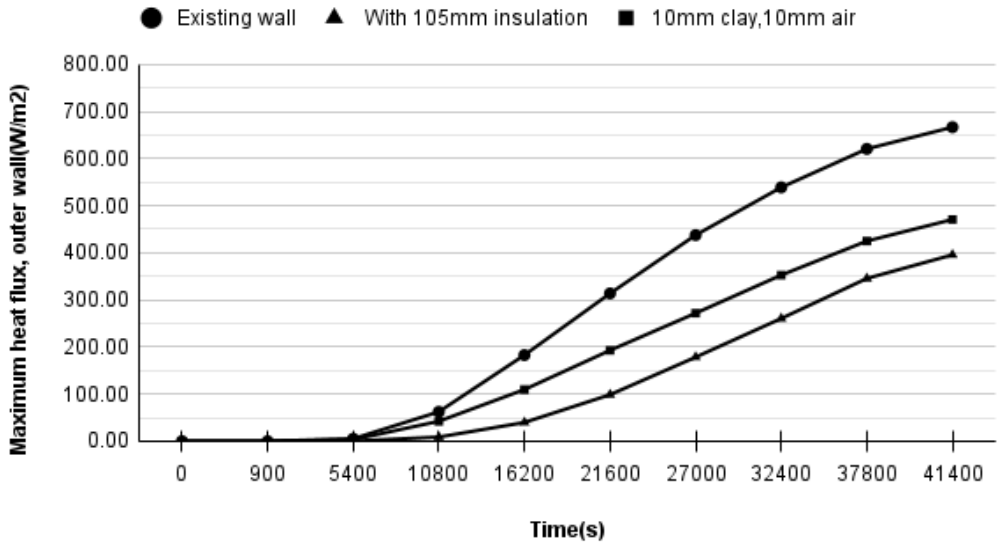

Figure 5.20: Comparison of outer wall heat flux at different times for the three models of wall

For the thickness of 40mm insulation of ceramic fibre blanket added, the maximum heat flux value can be reduced to 395.63 W/m^2. The reduction in the maximum heat flux on outer wall of furnace is 29.4% for clay-air gap combination while for the added 40 mm layer of insulation, the reduction in heat flux is 40.6%.

$\%\, reduction\ in\ heat\ flux_1 = \frac{666.68-470.67}{666.68} = 29.4\%$

$\%\, reduction\ in\ heat\ flux_2 = \frac{666.68-395.63}{666.68} = 40.6\%$

Though the reduction in the heat flux through the outer wall is more by the addition of the 4cm thick insulation layer, the reduction in the heat flux by the introduction of clay-air gap combination is more economical way of reduction of the heat flux from the outer wall. This is because, with an extra 40mm thick insulation added, more amount of heat is stored in the wall. While the addition of this extra layer of insulation outside the existing furnace wall ensures the reduction of heat loss from the outer wall of the furnace, it does not ensure that all the conserved heat is trapped inside the enclosure of furnace.

5.6 Economic analysis for the wall alterations

The two approaches of the wall alteration are analysed for the energy and hence cost savings. Both the approaches are low budget methods of altering the wall.

Table 5.6 Cost price for additional materials required for the furnace reconstruction

S.No.	Particulars	Rate	Cost (NRs)
1.	Clay,10mm (22kg)	55/kg	1936
2.	Cost of extra ceramic fibre blanket,40mm (23.2kg)	328/kg	7610
3.	Labour charge for furnace reconstruction (6 days)	3000/ (day)	18,000

The estimate of the clay for 10mm layer outside of the refractory wall is 22kg while for the 40mm insulation to be added 23.2kg is estimated with their price taken from ashaindia.com, the supplier from Pune, India. The energy and cost savings calculations for both the cases are shown below.

1) **Constant total thickness approach**

- The time for the internal environment of the furnace to reach 1075. $1°C$= 35,920s = 9.97 hrs
- Heat flux through the outer wall = 470.67W/m^2
- Total energy input for 9.97 hours = $11500\times\ 35920 = 413.08\ MJ$
- Energy saving = $476.1 - 413.08\ MJ = 63.02\ MJ$
- Units of electricity saved/cycle = $17.5\ units$
- Cost per unit = NRs 12
- Total cost saved/cycle = NRs 210

If only sintering process is carried out in this furnace and the furnace can be loaded every 5 days then the total cost saving in a year is

- Annual cost saving= $210 \times \frac{365}{5} = \text{NRs } 15{,}330$
- With the labour cost and other material cost remaining the same, the extra material needed is clay for the reconstruction of the furnace.
- Payback period $= \frac{Total\ investment}{Yearly\ saving} = \frac{1936}{15330} = 0.126yrs$

2) Variable total thickness approach

- The time for the internal environment of the furnace to reach $1075.1°C$= 37830s = 10.5 hrs
- Heat flux through the outer wall = 395.63W/m^2
- Total energy input for 9.97 hours = 11500$\times$ 37830 $= 436.88\ MJ$
- Energy saving = $476.1 - 436.88\ MJ = 39.22\ MJ$
- Units of electricity saved/cycle = $10.9\ units$
- Cost per unit = NRs 12
- Total cost saved/cycle = NRs 131

For cycle repeated in every 5 days

Annual cost saving=131$\times \frac{365}{5} = \text{NRs } 9{,}563$

With the labour cost and other material cost remaining the same, the extra material needed is 40mm thick insulation

- Payback period $= \frac{Total\ investment}{Yearly\ saving} = \frac{7610}{9563} = 0.795yrs$

The payback period for both the cases is less than a year. Moreover, in terms of cost wise the constant total thickness approach is better than the variable total thickness approach with payback period of only 0.126 years.

5.7 Selection of proper heating element

The suitable heating element for the furnace can be chosen on the basis of surface loading data of the Kanthal A wire. For the existing rated power of 11.5kW and 220V, the heating element design is done as follows:

Firstly the current is calculated from the power and voltage.

Current (I) $=$ P/V $=$ $11500/220 =$ 52.27A

The maximum working temperature of the Kanthal A wire is $1300°C$

From the data handbook of Kanthal A wire, the factor of resistance ((C_t) = 1.06 for $1300°C$.

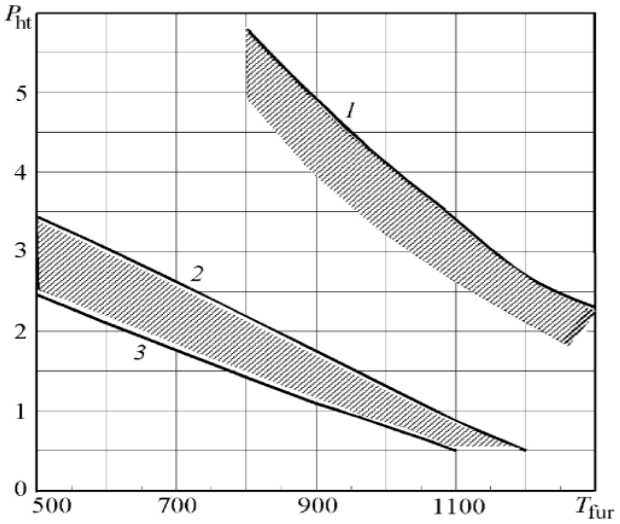

Figure 5.21: Surface loading data of (1) Kanthal wire (2) Nichrome wire (3) Platinum wire (Grinchuk, 2010)

The minimum surface loading of the Kanthal wire is taken, as W_d = 2 W/cm^2.

Hence, $\frac{cm^2}{\Omega} = \frac{I^2.C_t}{W_d} = \frac{((52.27)^2 \times 1.06}{2} = 1448.04$

Now, the closest value to 1448.04 is searched in the data handbook of the Kanthal A wire under the column of $\frac{cm^2}{\Omega}$.

The nearest value to 1448.04 is 1618 and the diameter corresponding to this value is 4.5mm. Hence, the suitable wire diameter from this method would be 4.5mm but the wire of 1.7mm diameter is being used at the experimental data collection location. As seen from the figure 5.22, the surface loading of the wire can be higher for the lower temperatures and it decreases as the temperature increases.

5.8 Verification of the power and energy consumed by the furnace

According to the data of OEFEN, a German company, that manufactures furnaces for ceramics, glass and solar cells, ("Furnaces for Ceramics, Glass Solar Cells," 2021) the chamber furnace of internal dimension of $(520 \times 630 \times 770)$mm^3 that operates on the maximum temperature of $1280°C$ has a power rating of 13.5kW. This furnace has a weight of 480kg and an internal volume of 250 litres. The furnace under study in this paper has comparable dimensions to that of the furnace mentioned above with the power rating of 11.5kW. The internal dimensions of the furnace of $(920 \times 640 \times 640)$mm^3 is also comparable. Hence, the power rating of the furnace is well within the accepted value with the standard furnace manufactured for heat treatment of ceramics.

CHAPTER SIX: CONCLUSIONS AND RECOMMENDATIONS

7.1 Conclusions

From the experimental study of the furnace, the following conclusions are drawn.

- The ceramics is heat treated inside the furnace until the temperature of the furnace environment reaches $1075°C$ during the sintering or second firing process. The heating rate of the clay based ceramics decreases gradually as the process proceeds towards the completion. The heating rate which is $3.53°C/\text{min}$ in the first step drops to only $0.80°C/\text{min}$ at the last time step of the process.
- The temperature of the outer wall of the furnace reaches around $113.2°C$. The temperature on the front wall of the furnace is higher than the other walls of the furnace. This temperature distribution on the outer wall of the furnace suggests that there are defects present on the furnace wall.

From the computational study of the heat transfer in a simplified model of electric resistance furnace that converged to a desired accuracy, the following conclusions are drawn.

- The temperature of the furnace outer wall reaches $96.86°C$ which is lower than the experimental value by around $16.33°C$. This temperature is higher by around $27°C$ from the industrial standards of below $70°C$ for heat treating and reheating furnaces. Hence, it can be deducted that there are defects on the furnace wall. Also, insulation of the furnace wall is insufficient and can be improved substantially to improve the performance of the furnace by reducing the heat loss from the walls.
- The average internal temperature of the furnace at process completion is $1132°C$.
- The average temperature of the object placed at the centre is $1087.2°C$, with the highest temperature on the side of the object facing the heating element to be $1144.3°C$ and lowest temperature on the central section to be $1026°C$.
- The replacement of 20mm insulation by a combination of 10mm clay and 10mm air gap combination adjacent to the refractory brick layer reduces the heat flux on the outer wall by 29.4%.
- The additional thickness of insulation of the ceramic fibre blanket to be added on the outside of existing furnace to meet the industrial standards or to obtain a temperature of below $70°C$ is 40mm.

7.2 Recommendations

In order to better understand the heat transfer phenomena occurring inside the electric resistance furnace, a detailed heat analysis of the furnace with appropriate loading can be done. The study can be done on the better and efficient way of loading the furnace as considerable heat is utilized to heat the materials that help in loading of the ceramic products. Furthermore, this study can be extended to do a detailed experimental as well as computational analysis of the cooling process of the heat treated ceramics. A study on the utilization of the hot air from the furnace in other low energy applications or the reutilization of the heated air can be done. Furnaces nowadays are equipped with temperature controller and other accessories to ensure the steady operation at soaking temperature. A study of the heat and temperature distribution on the workpiece after installation of temperature controller can be done. Other factors that affect the heat transfer through the walls of the furnace can be studied in detail. A heat flux sensor would really prove useful in the further study of furnace to quantify the heat loss occurring from the outer wall of furnace.

REFERENCES

Adhikari, U., Prajapati, B., In, A. B.-J. of I., & 2021, U. (2021). Performance evaluation and thermal analysis of pottery furnace in Thimi, Bhaktapur. *Nepjol.Info*. https://www.nepjol.info/index.php/jiee/article/view/39694

Awaji, H., Watanabe, T., & Nagano, Y. (1994). Compressive testing of ceramics. *Ceramics International*, *20*(3), 159–167. https://doi.org/10.1016/0272-8842(94)90034-5

C. Barry Carter, M. G. N. (1974). *Ceramic Materials_ Science and Engineering (2007, Springer)*.

Carvalho, M. O., & Nogueira, M. (1991). *Mathematical modeling of a heat transfer in an industrial glass furnace*. *m*.

Chook, K. C., & Tan, A. H. (2007). Identification of an electric resistance furnace. *IEEE Transactions on Instrumentation and Measurement*, *56*(6), 2262–2270. https://doi.org/10.1109/TIM.2007.907960

Colomer, G., Costa, M., Cònsul, R., & Oliva, A. (2004). Three-dimensional numerical simulation of convection and radiation in a differentially heated cavity using the discrete ordinates method. *International Journal of Heat and Mass Transfer*, *47*(2), 257–269. https://doi.org/10.1016/S0017-9310(03)00387-9

Davies, C. (1966). *Calculations in Furnace Technology: Division of Materials Science and Technology*. https://books.google.com.np/books?hl=en&lr=&id=PBASBQAAQBAJ&oi=fnd&pg=PP1&dq=Calculations+in+Furnace+Technology&ots=6VlgkUGfTK&sig=b7bUDtPG8oe2Au_6lTuz8bs_bns&redir_esc=y#v=onepage&q=Calculations in Furnace Technology&f=false

Dimitrov and Zhekov. (2014). *ANALYSIS OF THE APPROACHES FOR IMPROVEMENT OF THE ENERGY EFFICIENCY OF ELECTRIC RESISTANCE FURNACES*. – STUME Journals. https://stumejournals.com/journals/mtm/2014/12/31

Dimitrov, B., Tahrilov, H., & Nikolov, G. (2012). *Study and analysis of optimization approaches for insulation of an industrial grade furnace with electrical resistance*

heaters.

Dimitrov, B., & Yatchev, I. (2012). Study of high-temperature chamber-type electric resistance furnace and attainment of uniform temperature field. *2012 International Conference on Applied and Theoretical Electricity, ICATE 2012 - Proceedings*. https://doi.org/10.1109/ICATE.2012.6403448

Ferrer, S., Mezquita, A., Gomez-Tena, M. P., Machi, C., & Monfort, E. (2015). Estimation of the heat of reaction in traditional ceramic compositions. *Applied Clay Science*, *108*, 28–39. https://doi.org/10.1016/J.CLAY.2015.02.019

Fu, Z., Yu, X., Shang, H., Wang, Z., & Zhang, Z. (2019). A new modelling method for superalloy heating in resistance furnace using FLUENT. *International Journal of Heat and Mass Transfer*, *128*, 679–687. https://doi.org/10.1016/j.ijheatmasstransfer.2018.08.105

Furnaces for Ceramics, Glass Solar cells. (2021). *Thermoconcept*, 48. https://www.thermconcept.com/data/files/193/en/Oefen_fuer_Keramik_Glas_Solar_EN.pdf

Gao, M., Reid, C. N., Jahedi, M., & Li, Y. (2000). Estimating equilibration times and heating/cooling rates in heat treatment of workpieces with arbitrary geometry. *Journal of Materials Engineering and Performance*, *9*(1), 62–71. https://doi.org/10.1361/105994900770346295

Gołdasz, A., & Malinowski, Z. (2017). Identification of the Heat Transfer Coefficient at the Charge Surface Heated on the Chamber Furnace. *Archives of Metallurgy and Materials*, *62*(2), 509–513. https://doi.org/10.1515/amm-2017-0075

Grinchuk, P. S. (2010). Mathematical modeling of thermal operating regimes of electric resistance furnaces. *Journal of Engineering Physics and Thermophysics*, *83*(1), 30–40. https://doi.org/10.1007/s10891-010-0316-4

Heating Element Design Factors. (n.d.). Retrieved July 26, 2022, from https://www.heating-element-alloy.com/article/heating-element-design-factors.html

Hemmer, C., Polidori, G., & Popa, C. (2014). Temperature optimization of an electric heater by emissivity variation of heating elements. *Case Studies in Thermal Engineering*, *4*, 187–192. https://doi.org/10.1016/j.csite.2014.10.001

Indian Bureau of Energy Efficiency. (2015). *INSULATION AND REFRACTORIES*.

Janata. (1982). *Simplified mathematical models of heat transfer in continuous fuel-fired furnaces*. *53*(figure 2), 343–348.

Kang, J., Rong, Y. K., & Wang, W. (2004). Numerical simulation of heat transfer in loaded heat treatment furnaces. *Journal De Physique. IV : JP*, *120*, 545–553. https://doi.org/10.1051/JP4:2004120063

Lin, B., Liu, F., Zhang, X., Liu, L., & Zhu, X. (2011). Simulation Technology in the Sintering Process of Ceramics. In *Numerical Simulations - Applications, Examples and Theory*. https://doi.org/10.5772/13082

Mackenzie, B. R. C. (1982). *The Story of the Platinum-Wound Electric Resistance Furnace*. *4*, 175–183.

Mariños Rosado, D. J., Rojas Chávez, S. B., Amaro Gutierrez, J., Carvalho, J., Huaraz Rodriguez, M., & Armando Mendiburu Zevallos, A. (2020). *Reheating Furnaces in the Steel Industry: Reduction of Heat Transfer Losses By Analyzing the Types of Insulation Materials and Thickness in Each Layer*. *November*. https://doi.org/10.26678/abcm.encit2020.cit20-0015

Marlow, D. (1995). Mathematical modelling of the heat treatment in the continuous processing of steel strip. *U.S. Environmental University of Wollongong Thesis Collections*, *1*.

Norton, & Carter. (2019). *Ceramic Materials*. 9–25.

Richards, J. W. (2013). The electric melting furnace: The early history of the electric melting furnace and its development into various commercial types. *Journal of the American Institute of Electrical Engineers*, *39*(12), 1034–1036. https://doi.org/10.1109/JOAIEE.1920.6594644

Ritonga, W., Harahap, M. H., Putra Stevano, F. Y., & Rajagukguk, J. (2021). Design and construction of an electrical furnace chamber based on RERIH system for high temperature. *Journal of Physics: Conference Series*, *1819*(1). https://doi.org/10.1088/1742-6596/1819/1/012023

Shrestha, P. (2018). Challenges and Scopes of Pottery Industry. *Pravaha*, *24*(1), 147–158. https://doi.org/10.3126/PRAVAHA.V24I1.20234

Walton, R. R. (2000). Furnaces, Electric, Resistance Furnaces. *Kirk-Othmer Encyclopedia of Chemical Technology*. https://doi.org/10.1002/0471238961.1805190923011220.A01

Zhang, X. F., Lin, B., & Chen, S. H. (2008). Numerical simulation of temperature distribution during ceramic sintering. *Applied Mechanics and Materials*, *10–12*, 331–335. https://doi.org/10.4028/www.scientific.net/AMM.10-12.331

Appendix A:

Table A1: Material properties of the different materials

Material	**Thermodynamic properties**		
Refractory brick	Density(kg/m^3)	Thermal conductivity(W/m.K)	Specific heat(J/kg.K)
Fireclay, 2400	2400	1.34	800
Fireclay, 2080	2080	1.02	800
Fireclay,1760	1760	0.78	800
Fireclay,1440	1440	0.57	800
Fireclay,1280	1280	0.48	800
Insulation brick			
Diatomite solid	1090	0.25	1308
Diatomite porous	540	0.14	1250
Clay	560	0.3	878
Alumina	850	0.12-0.22	880
Silica	830	0.4	970
Hot Insulations			
Calcium silicate	260	0.08	960
Resin-bonded mineral wool	48-144	0.11	921
Ceramic fibre blanket	64-128	0.117	1070

Appendix B:

Table C1: Data handbook of Kanthal A wire used as the heating element.

KANTHAL A, AF, AE Wire

Standard stock items	Alloy	Diameter range mm	Resistivity Ωmm²m⁻¹	Density gcm⁻³
■	KANTHAL A	10.0-0.05	1.39	7.15
■	KANTHAL AF	10.0-0.10	1.39	7.15
–	KANTHAL AE	10.0-0.20	1.39	7.15

To obtain resistance at working temperature, multiply by the factor C_t in the following table:

°C	20	100	200	300	400	500	600	700	800	900	1000	1100	1200	1300
C_t	1.00	1.00	1.01	1.01	1.02	1.03	1.04	1.04	1.05	1.05	1.06	1.06	1.06	1.06

Diameter mm A	AF	at 20 °C Ω/m	Resistance cm²/Ω¹⁾ at 20 °C	Weight g/m	Surface area cm²/m	Cross sectional area mm²
10	10.0	0.0177	17751	562	314	78.
	8.25	0.0260	9968	382	259	53.5
	8.0	0.0277	9089	359	251	50.3
	7.5	0.0315	7489	316	236	44.2
	7.35	0.0328	7048	303	231	42.4
	7.0	0.0361	6089	275	220	38.5
	6.54	0.0414	4965	240	205	33.6
	6.5	0.0419	4875	237	204	33.2
	6.0	0.0492	3834	202	188	28.3
	5.83	0.0521	3517	191	183	26.7
	5.5	0.0585	2953	170	173	23.8
	5.2	0.0655	2496	152	163	21.2
	5.0	0.0708	2219	140	157	19.6
	4.75	0.0784	1902	127	149	17.7
	4.62	0.0829	1750	120	145	16.8
	4.5	0.0874	1618	114	141	15.9
	4.25	0.0980	1363	101	134	14.2
	4.11	0.105	1232	94.9	129	13.3
	4.0	0.111	1136	89.8	126	12.6
	3.75	0.126	936	79.0	118	11.0
	3.65	0.133	863	74.8	115	10.5
	3.5	0.144	761	68.8	110	9.62
	3.25	0.168	609	59.3	102	8.30
	3.2	0.173	582	57.5	101	8.04
	3.0	0.197	479	50.5	94.2	7.07
	2.9	0.210	433	47.2	91.1	6.61
	2.8	0.226	390	44.0	88.0	6.16
	2.6	0.262	312	38.0	81.7	5.31
	2.5	0.283	277	35.1	78.5	4.91
	2.4	0.307	245	32.3	75.4	4.52
	2.3	0.335	216	29.7	72.3	4.15
	2.25	0.350	202	28.4	70.7	3.98
	2.2	0.366	189	27.2	69.1	3.80
	2.0	0.442	142	22.5	62.8	3.14
	1.8	0.546	104	18.2	56.5	2.54
	1.7	0.612	87.2	16.2	53.4	2.27
	1.65	0.650	79.7	15.3	51.8	2.14
	1.6	0.691	72.7	14.4	50.3	2.01
	1.5	0.787	59.9	12.6	47.1	1.77
	1.4	0.903	48.7	11.0	44.0	1.54
	1.3	1.05	39.0	9.49	40.8	1.33
	1.2	1.23	30.7	8.09	37.7	1.13
	1.1	1.46	23.6	6.79	34.6	0.950
	1.0	1.77	17.8	5.62	31.4	0.785
	0.95	1.96	15.2	5.07	29.8	0.709
0.90	0.90	2.18	12.9	4.55	28.3	0.636
0.85	0.85	2.45	10.9	4.06	26.7	0.567
0.80	0.80	2.77	9.09	3.59	25.1	0.503
0.75	0.75	3.15	7.49	3.16	23.6	0.442
0.70	0.70	3.61	6.09	2.75	22.0	0.385
0.65	0.65	4.19	4.87	2.37	20.4	0.332
0.60	0.60	4.92	3.83	2.02	18.8	0.283
0.55	0.55	5.85	2.95	1.70	17.3	0.238
0.50	0.50	7.08	2.22	1.40	15.7	0.196
0.45	0.45	8.74	1.62	1.14	14.1	0.159
0.40	0.40	11.1	1.14	0.898	12.6	0.126
0.35	0.35	14.4	0.761	0.688	11.0	0.0962
0.30	0.30	19.7	0.479	0.505	9.42	0.0707
0.25		28.3	0.277	0.351	7.85	0.0491
0.20		44.2	0.142	0.225	6.28	0.0314
0.15		78.7	0.0599	0.126	4.71	0.0177

THERMAL CONDUCTIVITY

Temperature °C	50	600	800	1000	1200
Temperature °F	122	1112	1472	1832	2192
W m-1 K-1	11	20	22	26	27
Btu h-1ft-1°F-1	6.4	11.6	12.7	15.0	15.6

Table C2: Properties of Kanthal wire

SPECIFIC HEAT CAPACITY

Temperature °C	20	200	400	600	800	1000	1200
Temperature °F	68	392	752	1112	1472	1832	2192
kJ kg-1 K-1	0.46	0.56	0.63	0.75	0.71	0.72	0.74
Btu lb-1 °F-1	0.11	0.13	0.15	0.18	0.17	0.17	0.18

Melting point °C (°F)	1500 (2732)
Max continuous operating temperature in air °C (°F)	1300 (2372)
Magnetic properties	The material is magnetic up to approximately 600°C (1112°F) (Curie point).
Emissivity - fully oxidized material	0.70

PHYSICAL PROPERTIES

Density g/cm3 (lb/in3)	7.15 (0.258)
Electrical resistivity at 20°C Ω mm2/m (Ω circ. mil/ft)	1.39 (836)
Poisson's ratio	0.30

YOUNG'S MODULUS

Temperature °C	20	100	200	400	600	800	1000
Temperature °F	68	212	392	752	1112	1472	1832
GPa	220	210	205	190	170	150	130
Msi	32	30	30	28	25	22	19

TEMPERATURE FACTOR OF RESISTIVITY

Temperature °C	100	200	300	400	500	600	700	800	900	1000	1100	1200	130
Temperature °F	212	392	572	752	932	1112	1292	1472	1652	1832	2012	2192	237
Ct	1.00	1.01	1.01	1.02	1.03	1.04	1.04	1.05	1.05	1.06	1.06	1.06	1.0

COEFFICIENT OF THERMAL EXPANSION

Temperature °C (°F)	Thermal Expansion x 10-6/K (10-6 /°F)
20 - 250 (68-482)	11 (6.1)
20 - 500 (68-932)	12 (6.7)
20 - 750 (68-1382)	14 (7.8)
20 - 1000 (68-1832)	15 (8.3)

Automatic exhaust flap

Technical Data 900 °C and 1280 °C - Models

Model	T max [°C]	Inner dimensions [mm] Width x Depth x Height	Volume [l]	Outer dimensions [mm] Width x Depth x Height	Power [kW]	Voltage [V]	Weight [kg]
KK 100/09../12	900 / 1280	410 x 470 x 540	100	750 x 970 x 1640	6,6 / 8	400 V 3/N	320
KK 150/09../12	900 / 1280	460 x 470 x 690	150	800 x 950 x 1730	9 / 10,5	400 V 3/N	430
KK 200/09../12	900 / 1200	460 x 630 x 690	200	800 x 1110 x 1730	11 / 13,2	400 V 3/N	460
KK 250/09../12	900 / 1280	520 x 630 x 770	250	860 x 1110 x 1740	13,5 / 16,5	400 V 3/N	480
KK 330/09../12	900 / 1280	580 x 710 x 800	330	920 x 1190 x 1740	16,5 / 22	400 V 3/N	530
KK 480/09../12	900 / 1280	550 x 800 x 800	480	970 x 1250 x 1760	32	400 V 3/N	620
KK 600/09../12	900 / 1280	710 x 820 x 1030	600	1050 x 1300 x 1770	40	400 V 3/N	730
KK 750/09../12	900 / 1280	710 x 1020 x 1030	740	1050 x 1500 x 1770	50	400 V 3/N	780
KK 1000/09../12	900 / 1280	910 x 1005 x 1145	1060	1250 x 1490 x 1890	70	400 V 3/N	1150
KK 1500/09../12	900 / 1280	900 x 1200 x 1400	1510	1590 x 2090 x 2410	58 / 76	400 V 3/N	2250
KK 2000/09../12	900 / 1280	1000 x 1300 x 1500	1950	1690 x 2190 x 2510	76 / 110	400 V 3/N	2890
KK 2500/09../12	900 / 1280	1000 x 1500 x 1650	2480	1690 x 2390 x 2660	110 / 140	400 V 3/N	3000

Figure: Power rating of chamber furnace, OEFEN

Appendix C:

Figure: Electric resistance furnace at Everest Pottery

Figure: A fully loaded furnace ready for operation

Appendix D:

MATLAB CODE: (By Dr. S. Han, Sep 9, 2008)

```
%tran1d.m. Transient,1-dimensional conduction
Finite volume formulation
%using matlab program.
%%%%%%%%%%%%%%%%%%%%%%%%
%%%specify the number of control volumes
n=18; % number of control volumes
maxiter = 40; % maximum number of iteration in each time step. set large for steady state
np1 = n+1;
np2 = n+2;
np3 = n+3;
%f = 1; %weighting function = 1 (fully-implicit);= 1/2 (Crank-Nicolson); = 0, (explicit)
%assign time step and maximum time
tstop = 41400; %% time to stop calculation
dt = 30; %% time step. set dt = 1.0e10 for steady state
mwrite = 1; %if dt>tstop mwrite must be set to 0.
%%define calculation domain
tl = 0.180; %total length of medium
delx = tl/n; % control volume size
dx = ones(np2);
dx = delx*dx;
%%replace fictitious boundary volume size to small value
dx(1) = 1.0e-10;
dx(np2) = 1.0e-10;
%%assign x-coordinate
x(1) = 0;
for m = 1:np2
 x(m+1) = x(m)+dx(m);
end
%%define cross-sectional area
%ac = ones(1,np3);%cross-sectional area
```

```
for i = 1:np3
 ac(i) = 0.4674; %constant cross section, dia = 0.0025 m
end
%time derivitive test
plotte = [];
f = 0;
for j = 1:3% weighting factor choice
%% prescribe initial temperatures for all control volumes
for i = 1:np2
 te0(i) = 25;
 te(i) = te0(i);
 tep(i) = te(i);
end
%%%%%%%%%%%%%%%%%%%%%%%% time loop begins here
t= 0; % starting time
iwrite = 1; % print out counter, iwrite<mwrite means skip print out
while t<tstop % calculation continues until t>tstop
%iteration for convergence
iter = 0; % set iteration counter in each time step
iflag = 1; % iflag = 1 means convergence not reached
%% iteration loop for the convergence in each time step
while iflag ==1 % end is at the end of program *********
%prescribe thermal conductivity, density and specific heat
 for i = 1:np2
 tk(i) = 0.1114; %%conductivity
 ro(i) = 397.611; %%density
 cp(i) = 948.611; %%specific heat capacity
 end
%%% prescribe boundary temperature
 te(1) = 1300;%at the left boundary given temperature
 te(np2) = te0(np2); %far away boundary
%% evaluate the diffusion conductance and source terms
for i= 2:np1
%%% diffusion conductance
```

```
 ke= tk(i)*tk(i+1)*(dx(i)+dx(i+1))/...
 (dx(i)*tk(i+1) + dx(i+1)*tk(i)); % east interface conductivity
 de=2.0*ke*ac(i+1)/(dx(i)+dx(i+1)); % east side diffusion conductance
%
 kw=tk(i)*tk(i-1)*(dx(i) + dx(i-1))/...
 (dx(i-1)*tk(i) + dx(i)*tk(i-1)); %west interface conductivity
 dw=2.0*kw*ac(i)/(dx(i-1) + dx(i));%west side diffusion conductance
%% time derivitive selection
 ae= f*de;
 aw= f*dw;
%% linearized source term evaluation
 sp= 0;
 sc= 0;
 vol= 0.5*(ac(i)+ac(i+1))*dx(i); % volume of cv
 a0= ro(i)*cp(i)*vol/dt; %% this term is zero for steady state
 ap= ae+aw+a0-f*sp*vol;
 b= sc*vol+de*(1-f)*te0(i+1)+dw*(1-f)*te0(i-1)+...
 (a0-(1-f)*de-(1-f)*dw+sp*(1-f)*vol)*te0(i);
%% setting coefficients for tdma matrix
 ta(i)= ap;
 tb(i)= ae;
 tc(i)= aw;
 td(i)= b;
%incorporate boundary conditions
 if i== 2
 td(i)= td(i)+aw*te(1); %at x=0
 elseif i== np1
 td(i)= td(i)+ae*te(np2); %at x=L
 end
end
%% solve the simultaneous equations by using tdma %%
nq= n;
nqp1= nq+1;
nqm1= nq-1;
```

```
%% forward substitution
beta(2)= tb(2)/ta(2);
alpa(2)= td(2)/ta(2);
for i= 3:nqp1
 beta(i)= tb(i)/(ta(i)-tc(i)*beta(i-1));
 alpa(i)= (td(i)+tc(i)*alpa(i-1))/...
 (ta(i)-tc(i)*beta(i-1));
end
%%backward substitution
dum(nqp1)= alpa(nqp1);
for j= 1:nqm1
 i= nqp1-j;
 dum(i)= beta(i)*dum(i+1)+alpa(i);
end
%end of tdma%%%%%%%%%update the temperature
for i=2:np1
 te(i)= dum(i);
end
%%%%%%%%%%%%%%%%%%%%%%%%%%%%%%%%%%%%%%%%%%%%
%%%%%%%%%%%%
% check the convergence
errote= ones(1,np2); %initialze error
for i= 1:np2
 errote(1,i)= abs(te(1,i)-tep(1,i))/te(1,i);
end
error= 1.0e-6; %prescribed error tolerance
 if (max(errote)>error) %%solution not converged
 iter= iter+1; %increase the iteration counter
 tep= te; % update the guessed value
 iflag= 1; % keep the flag red
 else
 iflag= 0; % solution converged, flag is green
 end
 if iter>maxiter % need to increase maxiter
```

```
 break
 end
end % this end goes with the while iflag==1 at the top   ********
%%solution converged
%%advance to the next time level and reinitialize the temperature
t= t+dt; %increase time
for i= 1:np2
 te0(i)= te(i); %reinitialize temperature
 tep(i)= te0(i);
end
%write the results at this time?
if iwrite>mwrite
%print the results at selected time interval
fprintf('iteration number is %i \n',iter)
iwrite= 0;
end
iwrite= iwrite+1;
end %this end goes with while t<tstop%%%%%%%%%%%%%%%%time loop
%%%%%%%%%%%%%%%%%%%%%%%%%%%%%%%%%%%%%%%%%%%%%%%%%%%%%%%%%%%
%%%plot at the end of calculation
plotte= [plotte te'];
f= f+0.5;
end %this goes with weighting factor f
% plot the result x.vs.te
% locate the midpoint of control volumes
for i= 1:np2
 xc(i)= 0.5*(x(i)+x(i+1));
end
%exact solution
alpha= tk(1)/(ro(1)*cp(1)); %thermal diffusivity
for i= 1:np2
 t1= erf(xc(i)/(2*sqrt(alpha*t)));
teexact(i)= te(1) + (te(np2)-te(1))*t1;
end
```

```
%
plot(xc,teexact,'-',xc,plotte(:,1),'-o',xc,plotte(:,2),'--x',xc,plotte(:,3),':*')
legend ('exact','f=0', 'f=1/2', 'f=1')
title ('1D Transient heat conduction through wall'), xlabel('Thickness of the wall,m'),
ylabel ('Temperature ,degree C')
grid on
```